

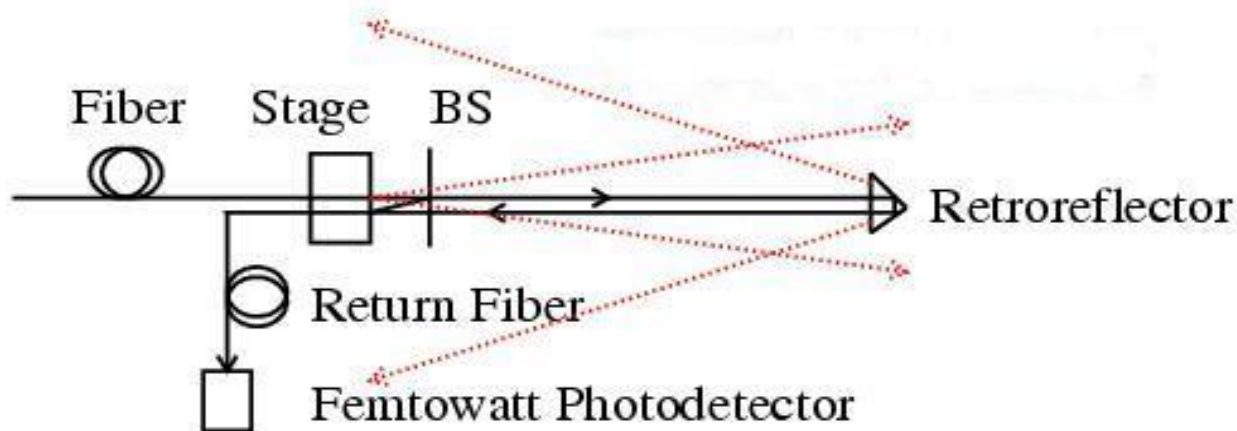
# Frequency Scanned Interferometry for ILC Tracker and Final Focus Magnet Alignment

Haijun Yang, Tianxiang Chen, Keith Riles  
University of Michigan, Ann Arbor

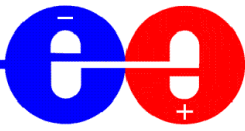
APS/DPF 2011, Brown University  
Rhode Island, August 9-13, 2011

- ➔ Introduction of Frequency Scanned Interferometry (FSI) method
- ➔ Review of improvements & measurements of FSI demonstration systems
  - ❑ Implementation of dual-laser technique
  - ❑ Results of measurements – estimated precision
  - ❑ Cross checks
- ➔ Current work on FSI with dual-channel system
- ➔ Summary

- ❑ Measure hundreds of absolute point-to-point distances of tracker elements in 3 dimensions by using an array of optical beams split from a central laser.
- ❑ Absolute distances are determined by scanning the laser frequency and counting interference fringes.
- ❑ Grid of reference points overdetermined → Infer tracker distortions



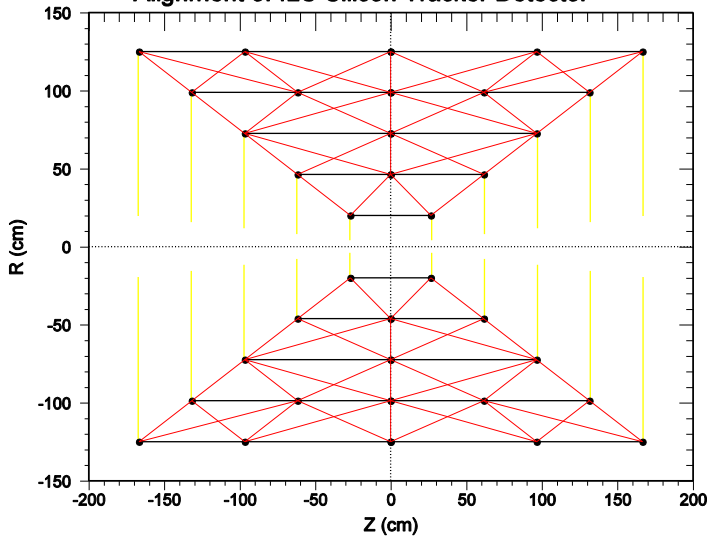
- ❑ Technique pioneered by Oxford U. group for ATLAS SCT detector



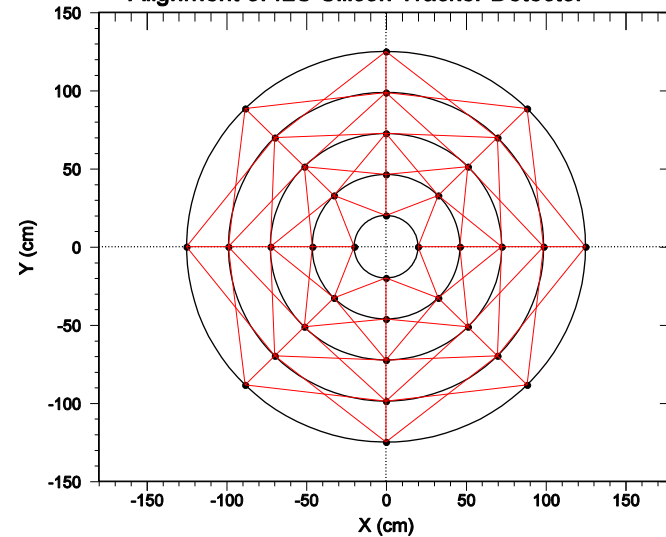
# A Possible SiD Tracker Alignment



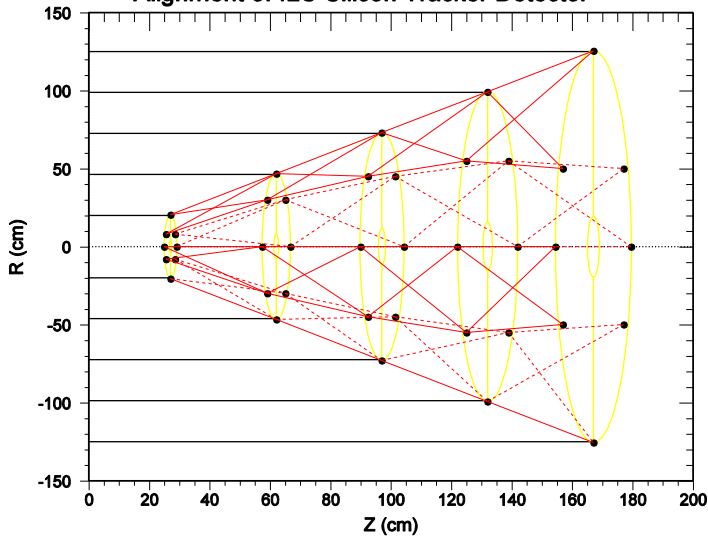
Alignment of ILC Silicon Tracker Detector



Alignment of ILC Silicon Tracker Detector



Alignment of ILC Silicon Tracker Detector



752 point-to-point distance measurements  
( Goal:  $\sigma_{\text{distance}} < 1 \mu\text{m}$  )

- The measured distance can be expressed by

$$R = \frac{c\Delta N}{2\bar{n}_g \Delta \nu} + \text{constant end corrections}$$

*c - speed of light,  $\Delta N$  – No. of fringes,  $\Delta \nu$  - scanned frequency  
 $\bar{n}_g$  – average refractive index of ambient atmosphere*

- Assuming the error of refractive index is small, the measured precision is given by:

$$(\sigma_R / R)^2 = (\sigma_{\Delta N} / \Delta N)^2 + (\sigma_{\Delta \nu} / \Delta \nu)^2$$

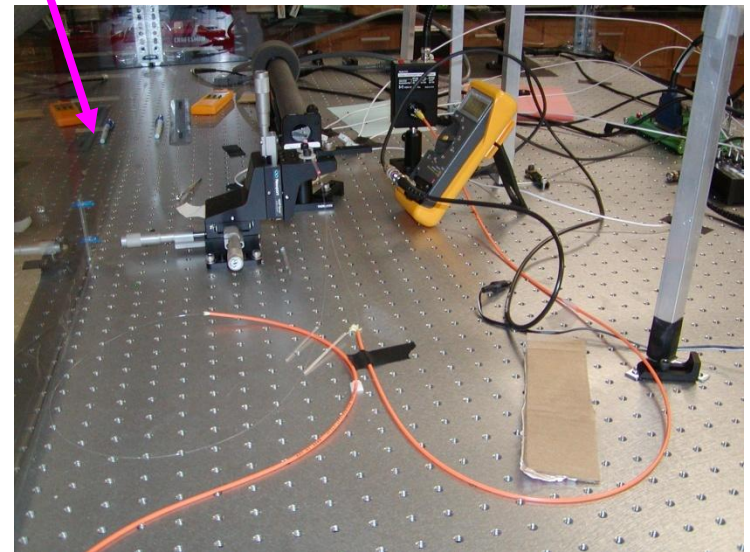
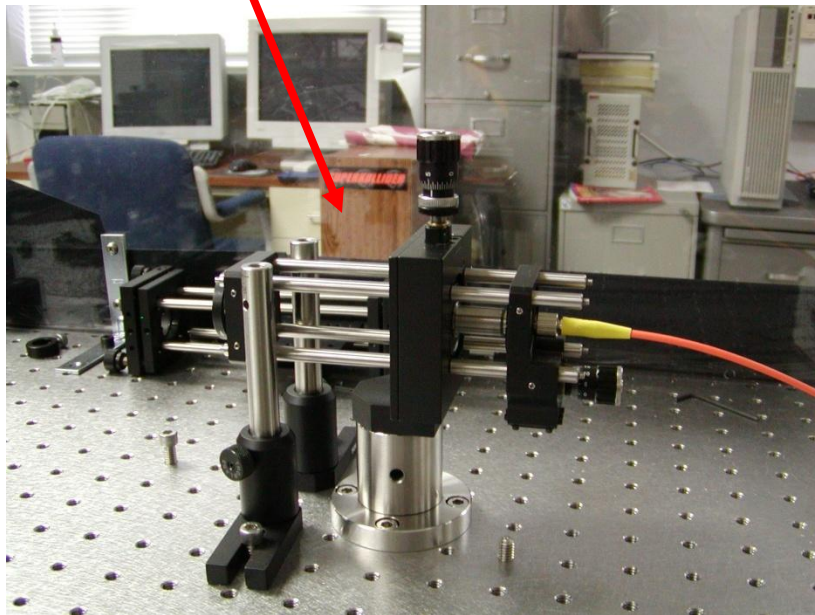
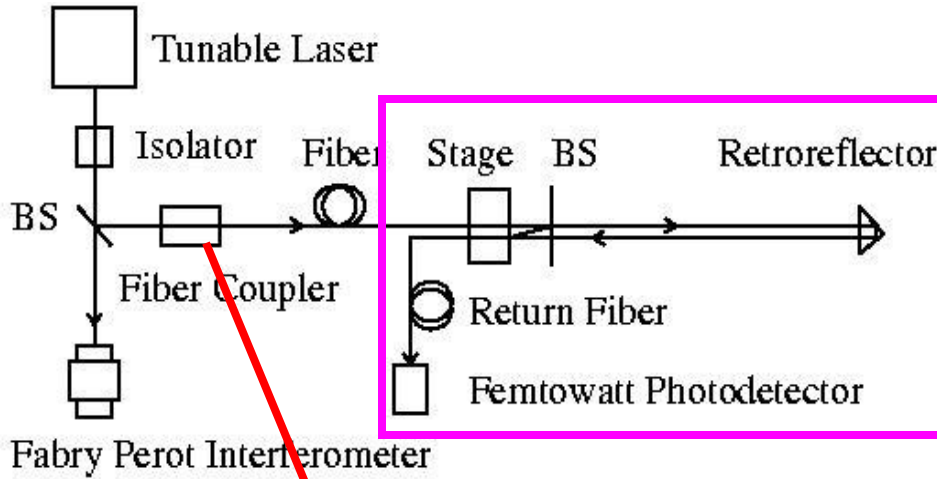
*Example:  $R = 1.0$  m,  $\Delta \nu = 6.6$  THz,  $\Delta N \sim 2R\Delta \nu / c = 44000$   
 To obtain  $\sigma_R \cong 1.0$   $\mu$ m, Requirements:  $\sigma_{\Delta N} \sim 0.02$ ,  $\sigma_{\Delta \nu} \sim 3$  MHz*

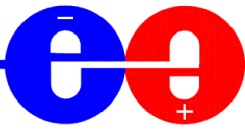
## Previous reports:

- FSI-I – Single-laser demonstration with air transport of beam
- FSI-II – Single-laser measurements with fiber transport
  - Results published in *Applied Optics*, **44**, 3937-44 (2005)  
Results (~ 50 nm) well within desired precision,  
but only for well controlled laboratory conditions
- FSI-III – Dual-laser measurements with fiber transport
  - Results published in *Nucl. Inst. & Meth. A* **575**, 395(2007)  
More realistic detector conditions (~ 0.2 microns)



# FSI with Optical Fibers (II)



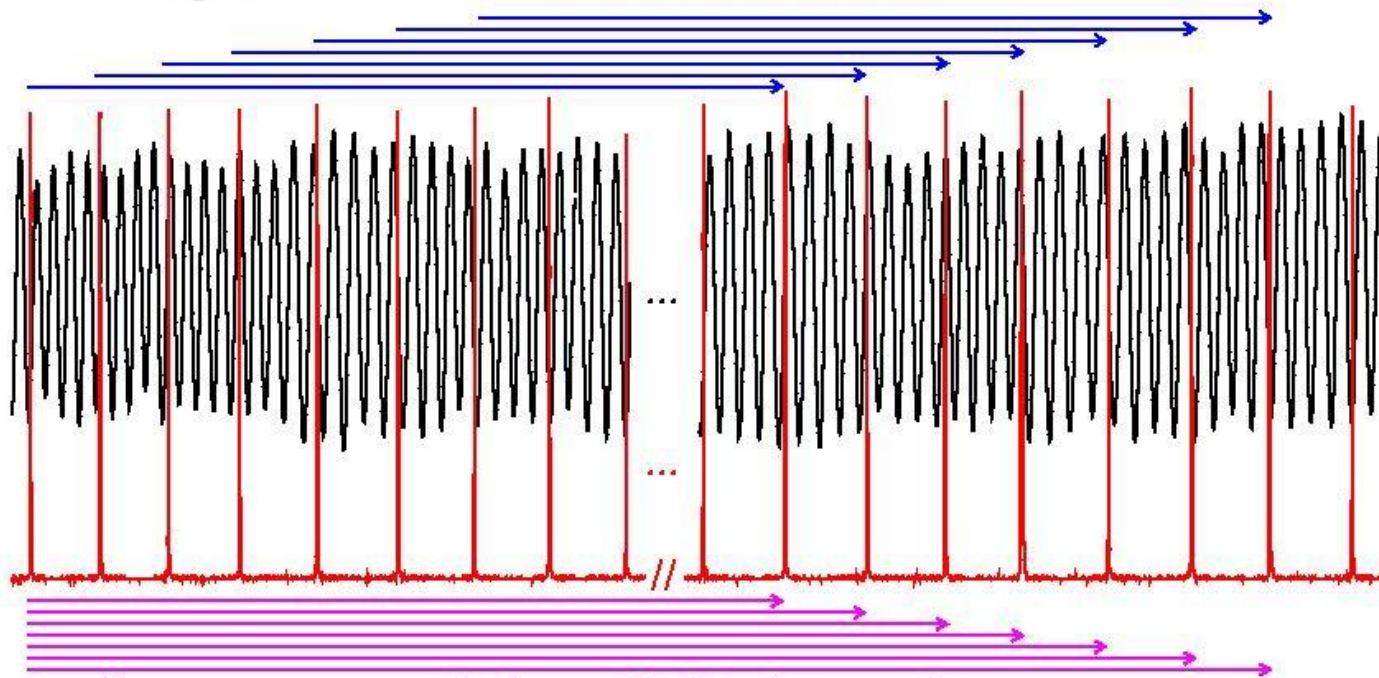


# Two Measurement Techniques



→ Fix the measurement window size ( $t-t_0$ ) and shift the window one F-P peak forward each time to make a set of distance measurements. The average value of all measurements is taken to be the final measured distance of the scan.

slip measurement window with fixed size



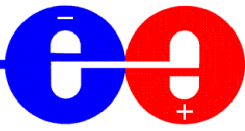
← Interference Fringes

← F-P Peaks  
FSR=1.5 GHz

slip measurement window with fixed start point

→ If  $t_0$  is fixed, the measurement window size is enlarged one F-P peak for each shift. An oscillation of a set of measured OPD reflects the amplitude and frequency of vibration.





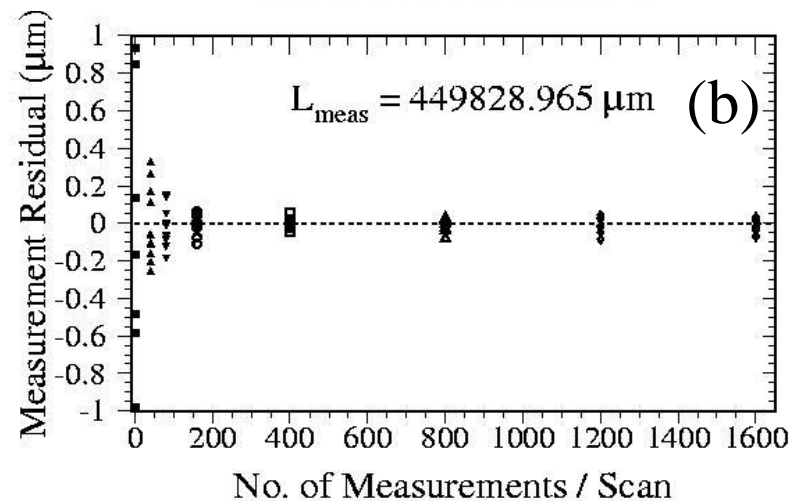
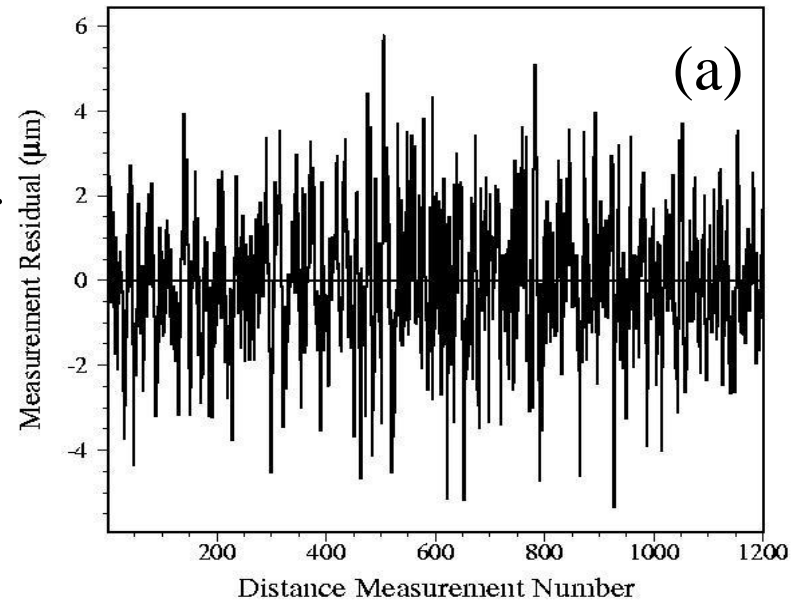
- The scanning rate was 0.5 nm/s and the sampling rate was 125 KS/s.
- The measurement residual versus the No. of measurements/scan shown in Fig.,
  - (a) for one typical scan,
  - (b) for 10 sequential scans.

→ It can be seen that the distance errors decrease with increasing  $N_{\text{meas}}$ .

$N_{\text{meas}}=1$ , precision=1.1  $\mu\text{m}$  (RMS)

$N_{\text{meas}}=1200$ , precision=41 nm (RMS)

→ Multiple-distance measurement technique is well suited for reducing vibration effects and uncertainties from fringe & frequency determination, BUT not good for drift errors such as thermal drift (needs dual-laser scanning technique).



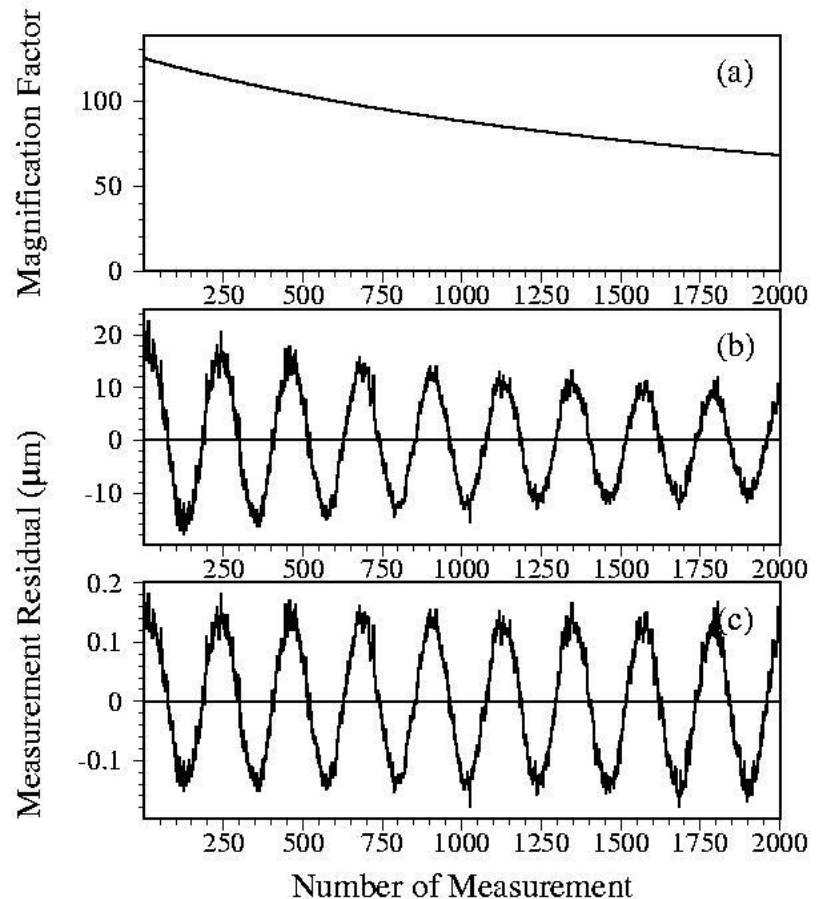
- A PZT transducer was employed to produce controlled vibration of the retroreflector,  $f_{\text{vib}} = 1.01 \pm 0.01$  Hz,  $\text{amp}_{\text{vib}} = 0.14 \pm 0.02$   $\mu\text{m}$

- Magnification factor  $\Omega = v/\Delta v$  for each distance measurement depends on the scanned frequency of the laser beam in the measurement window with smaller  $\Omega$  for larger window - plot(a). Since the vibration is magnified by  $\Omega$  for FSI during the scan, the expected reconstructed vibration amplitude is  $\sim 10.0$   $\mu\text{m}$  assuming  $\Omega \sim 70$  - plot(b).

→ The extracted true vibration - plot(c)

$$f_{\text{vib}} = 1.007 \pm 0.0001 \text{ Hz,}$$

$$\text{amp}_{\text{vib}} = 0.138 \pm 0.0003 \mu\text{m}$$



- Cannot count on precisely controlled conditions in ILC detector tracker.
- Thermal fluctuations and drifts likely
  - Refraction index and inferred distance affected
- Can measure temperature, pressure, humidity, etc. and apply empirical formulae, but preferable to measure effects directly and cancel these effects
- Use dual-laser technique (Invented by Oxford ATLAS group):
  - Two independent lasers alternately chopped
  - Frequency scanning over same range but with opposite slope

# Dual-Laser FSI (III)

→ A dual-laser FSI (Oxford ATLAS method) has been implemented with optical choppers.

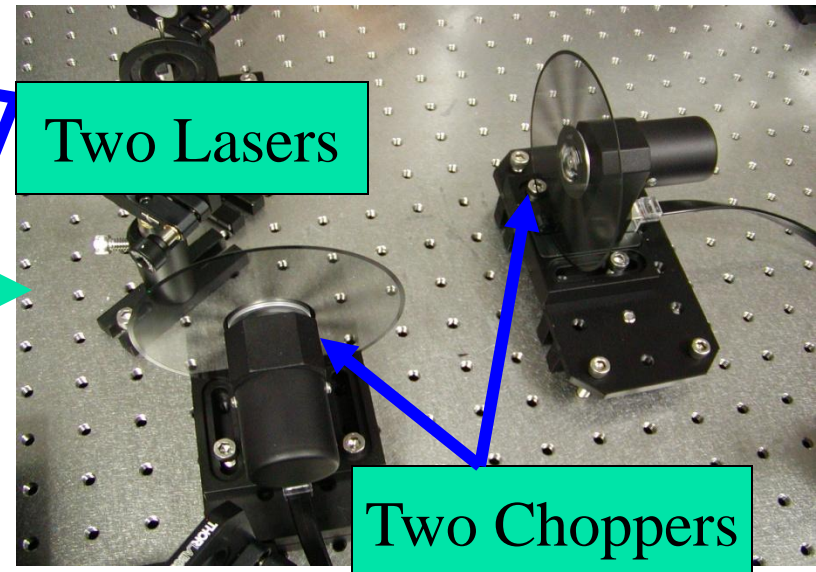
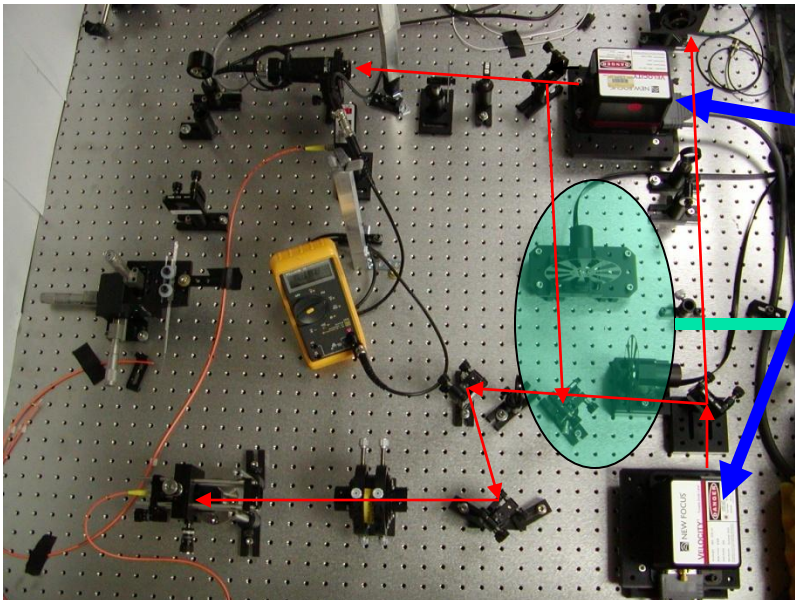
$$\text{Laser \#1: } D_1 = D_{\text{true}} + \Omega_1 \varepsilon_1$$

$$\text{Laser \#2: } D_2 = D_{\text{true}} + \Omega_2 \varepsilon_2$$

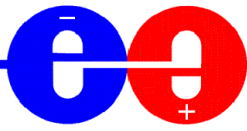
$$\text{Drift errors: } \varepsilon_1 \approx \varepsilon_2 = \varepsilon$$

$$D_{\text{true}} = (D_2 - \rho D_1) / (1 - \rho),$$

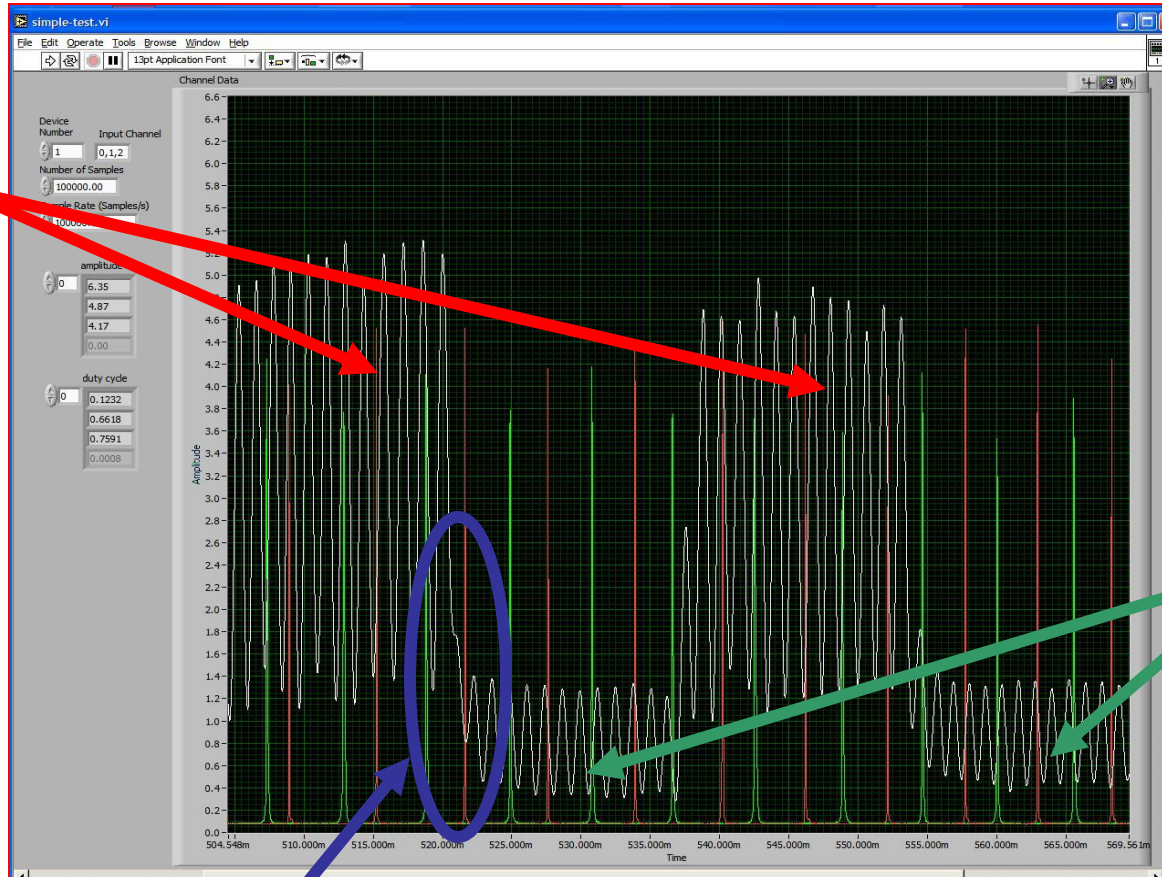
Where  $\rho = \Omega_2 / \Omega_1 \sim -1$  if two lasers are operating in opposite direction







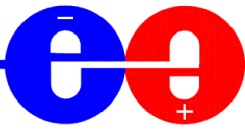
# Fringes & F-P Peaks (dual-laser)



Laser-1

Laser-2

Chopper edge effects and low photodiode duty cycle per laser complicate measurement.

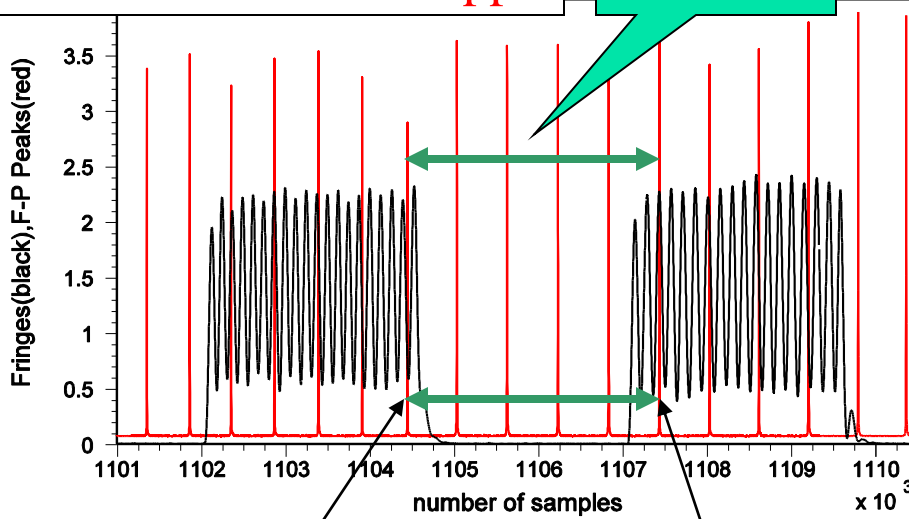


# Fringe Interpolating Technique



Laser #1 data with chopper

5 FSRs

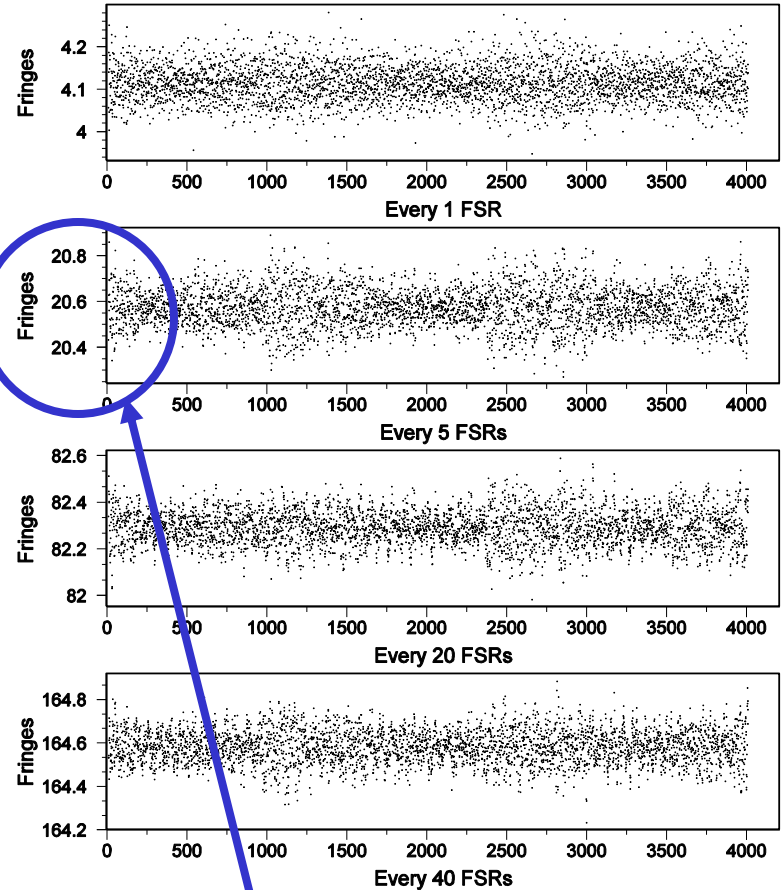


Fringe phase =  $I + \Delta I$

Fringe phase =  $J + \Delta J$

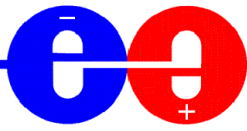
Fringe correction ( $N_{corr}$ ) must satisfy:  
 $minimize | N_{corr} + (J + \Delta J) - (I + \Delta I) - N_{average} |$   
 Where,  $N_{corr}$  is integer number,  $N_{average}$  is  
 expected average fringe numbers (real) for the  
 given number of FSRs.

Laser #1 data without chopper



Expected fringes for 5 FSRs



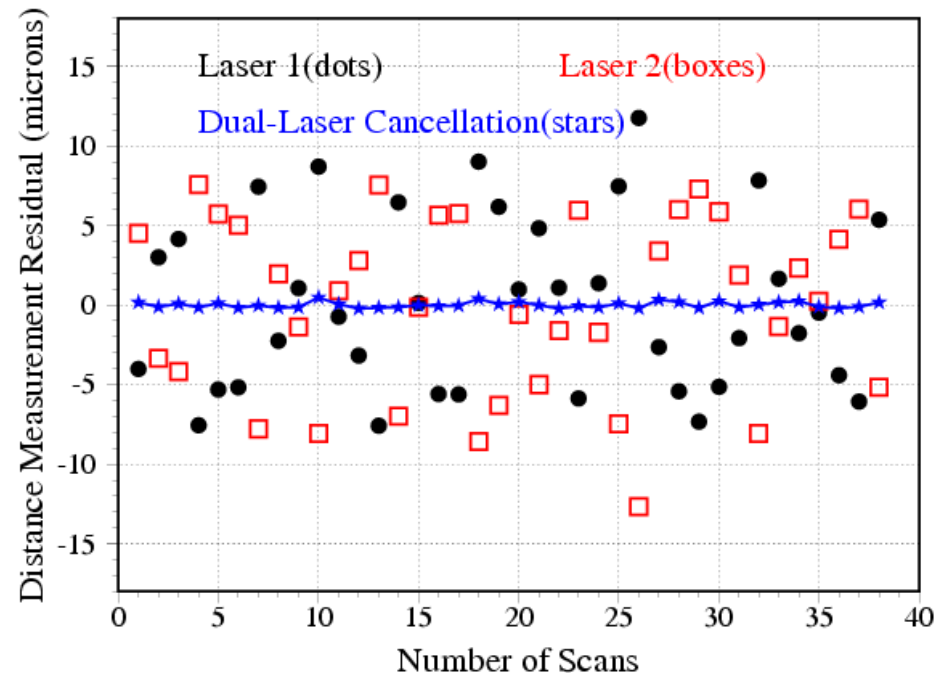


- Distance Measurement Precision ( $\sim 41.1384$  cm)  
Laser #1 or #2 only : Precision (RMS) = 3 ~ 7 microns
- Combining multi-distance-measurement and dual-laser scanning techniques to reduce and cancel interference fringe uncertainties, vibration and drift errors  
Dual-laser precision (RMS)  $\sim 0.20$  microns under realistic conditions

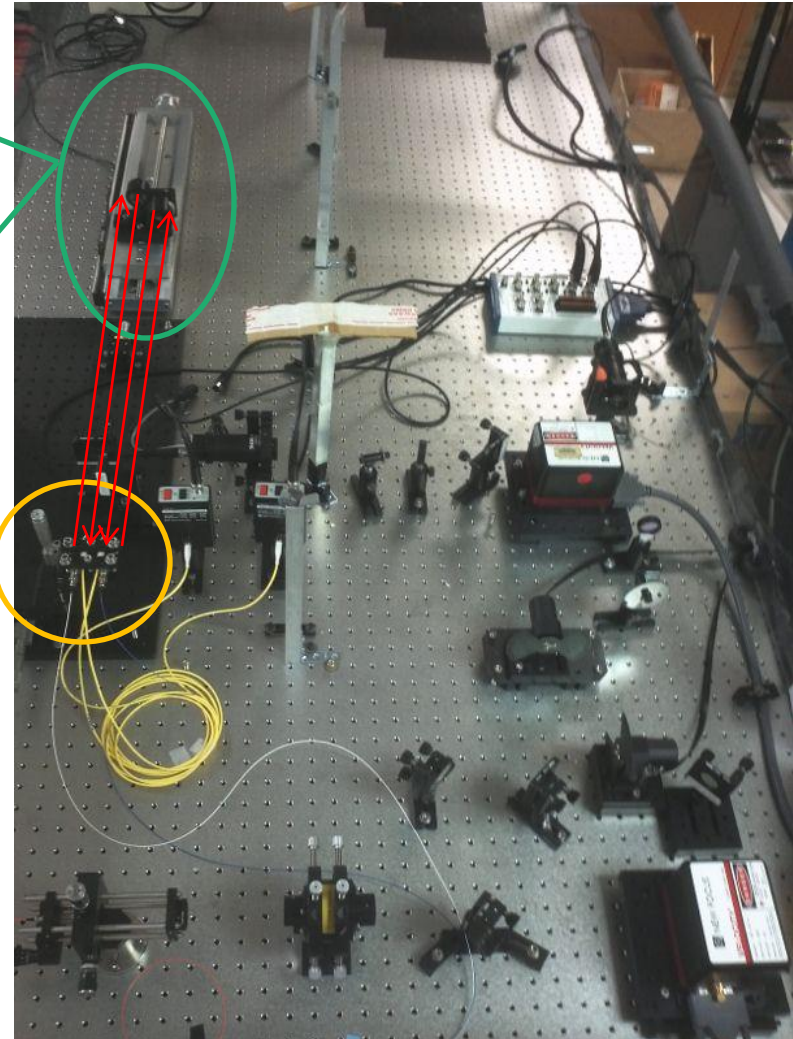
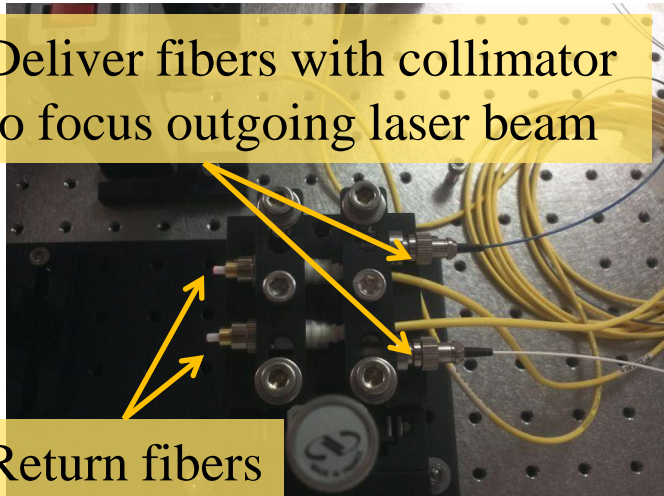
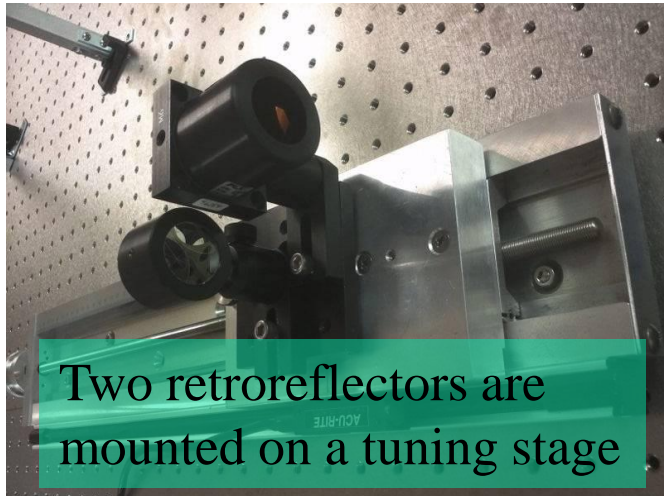
→ A 2<sup>nd</sup> publication:

“High-precision absolute distance measurement using dual-laser frequency scanned interferometry under realistic conditions”,

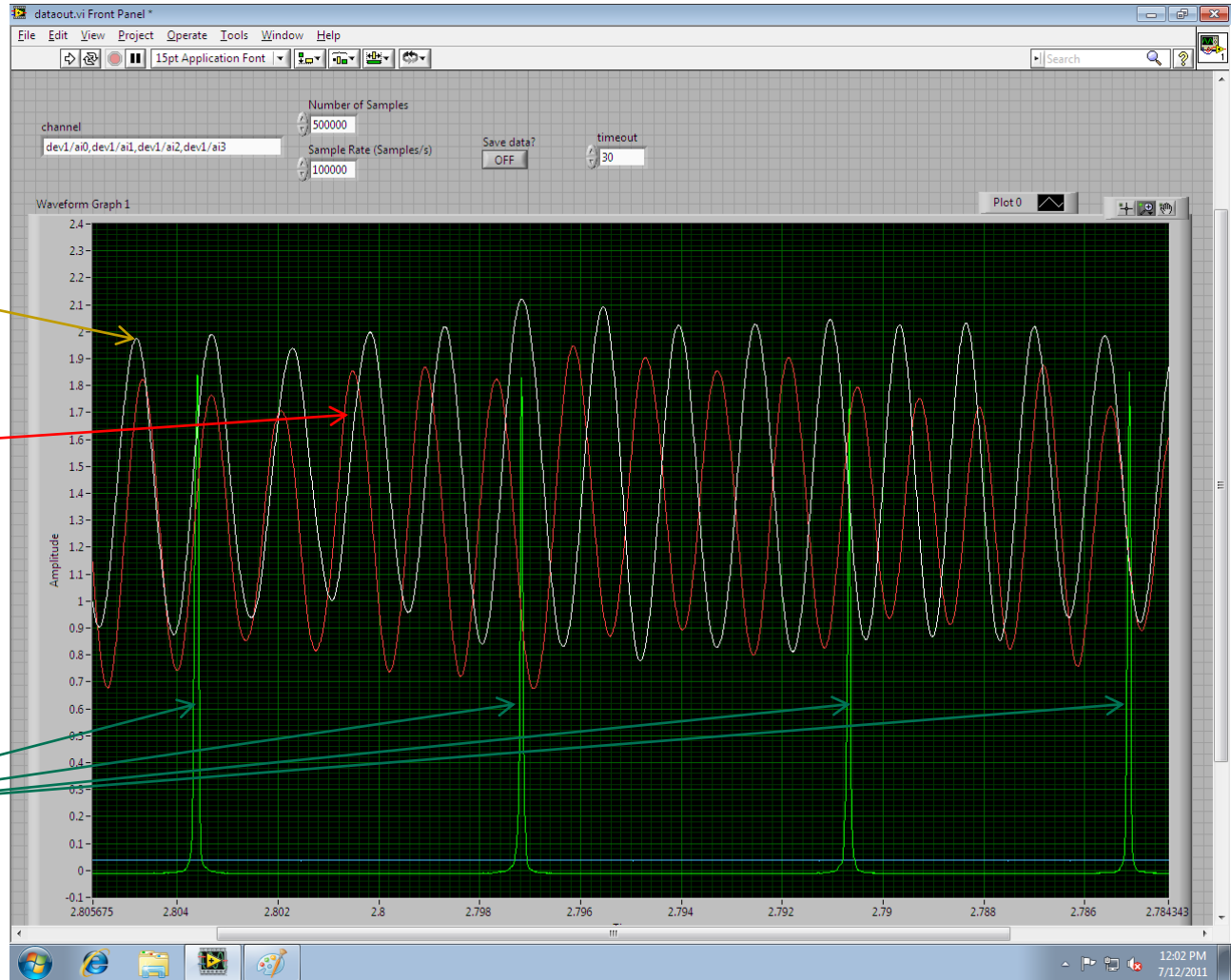
[Physics/0609187],  
Nucl. Inst. & Meth. A575, 395(2007)



We are implementing dual-channel fed by an optical fiber splitter



## Fabry-Perot peaks and interference fringes of two FSI channels



FSI Channel-1

FSI Channel-2

Fabry-Perot Peaks  
1.5 GHz / FSR

- Cross-check the distance measurements with two FSI channels using single laser.
  
- Using a tuning stage to change the position of two retroreflectors simultaneously by amount of  $(10 \pm 2)$  microns, and check FSI performance. Laser #1, 10 full scan data for each independent test ( $R_{\text{dist}} \sim 56$  cm)
  - $dR(\text{ch-1}) = 10.06 \pm 0.32$  microns,  $dR(\text{ch-2}) = 9.31 \pm 0.33$  microns
  - $dR(\text{ch-1}) = 10.63 \pm 0.55$  microns,  $dR(\text{ch-2}) = 10.19 \pm 0.51$  microns
  - $dR(\text{ch-1}) = 11.44 \pm 0.70$  microns,  $dR(\text{ch-2}) = 12.69 \pm 0.67$  microns
  
- Using a tuning stage to change large amount  $(650 \pm 5)$  microns, Laser #1, 10 full scan data for test
  - $dR(\text{ch-1}) = 647.60 \pm 1.43$  microns,  $dR(\text{ch-2}) = 646.66 \pm 0.71$  microns

➔ **Several FSI demonstration systems with increasing realism have been implemented, achievable distance measurement precision are quite promising (better than ~ 1 micron)**

➔ **Ongoing work:**

**Multiple channels:**

- dual-channel system are operating, 4-8 channels are in preparation

**Simulations (under development):**

- To determine SiD tracking component positions, rotations (pitch / roll / yaw), and internal distortions
- To evaluate the impact of distortion of silicon ladder on charged track momentum reconstruction

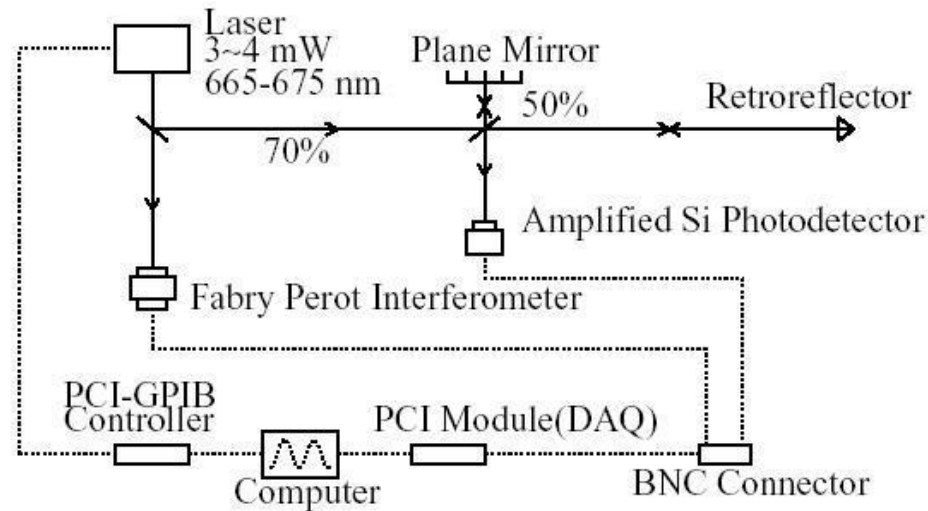
**Miniaturization:** To minimize the material mounted in the detector

➔ **Other applications:**

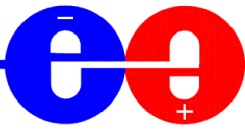
Planning to apply FSI method to final focus magnets alignment for SiD



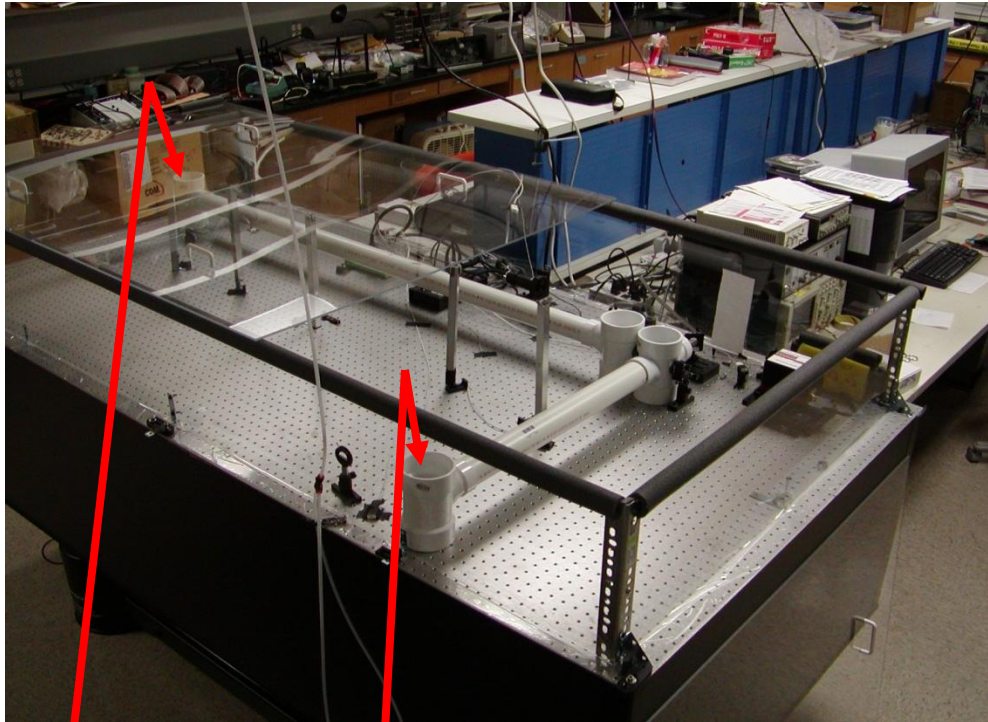




- ★ **Tunable Laser: New Focus Velocity 6308, 3-4 mW, 665.1-675.2 nm.**
- ★ **Retroreflector: Edmund, D=1", angle tolerance: ±3 arc seconds.**
- ★ **Photodiode: Thorlabs PDA55, DC-10MHz, Amplified Si Detector, 5 Gain Settings.**
- ★ **Thorlabs Fabry-Perot Interferometer SA200, high finesse(>200) to determine the relative frequency precisely, Free Spectral Range (FSR) is 1.5 GHz, with peak FWHM of 7.5 MHz.**
- ★ **Thermistors and hygrometer are used to monitor temperature and humidity respectively.**
- ★ **PCI Card: NI-PCI-6110, 5 MS/s/ch, 12-bit simultaneous sampling DAQ.**
- ★ **PCI-GPIB Card: NI-488.2, served as remote controller of laser.**
- ★ **Computers: 1 for DAQ and laser control, 3 for analysis.**



# FSI Demonstration System (I)



Photodetector

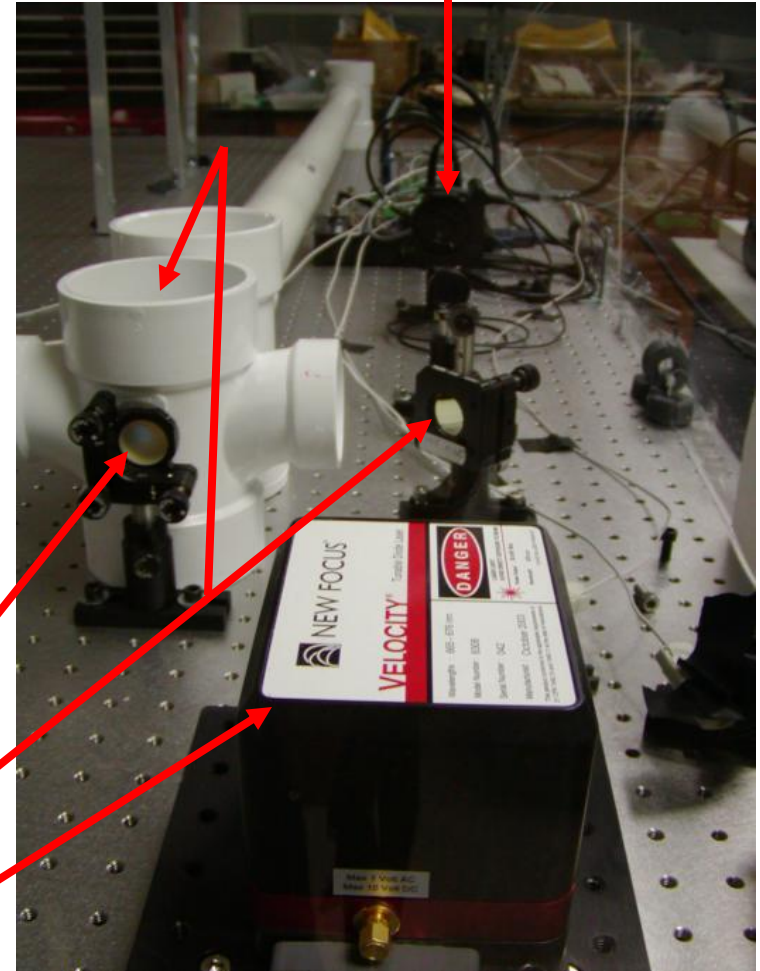
Retroreflector

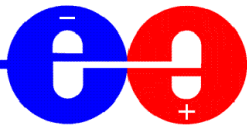
Mirror

Beamsplitters

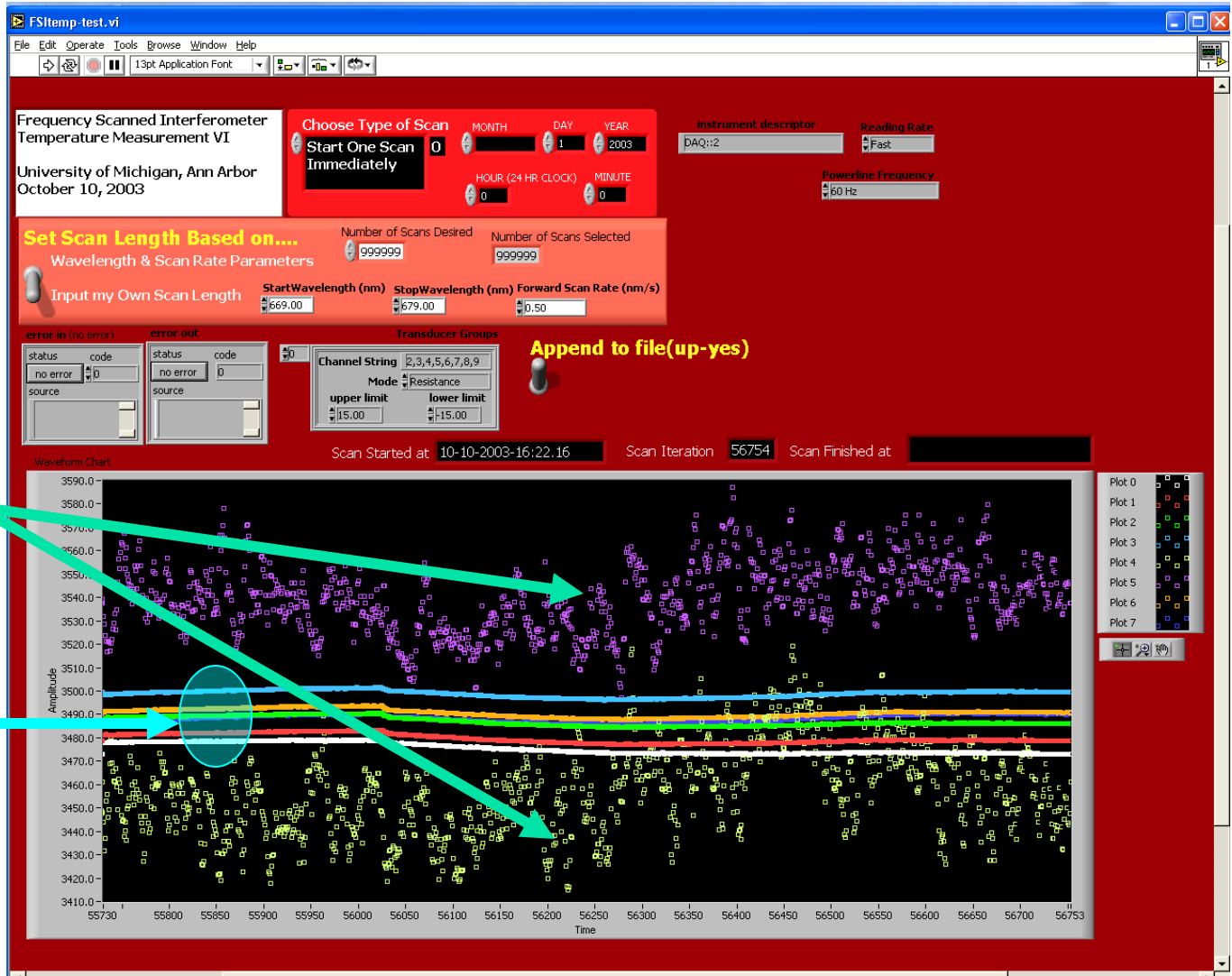
Laser

Fabry-Perot Interferometer





# Temperature Measurements



Outside of Box

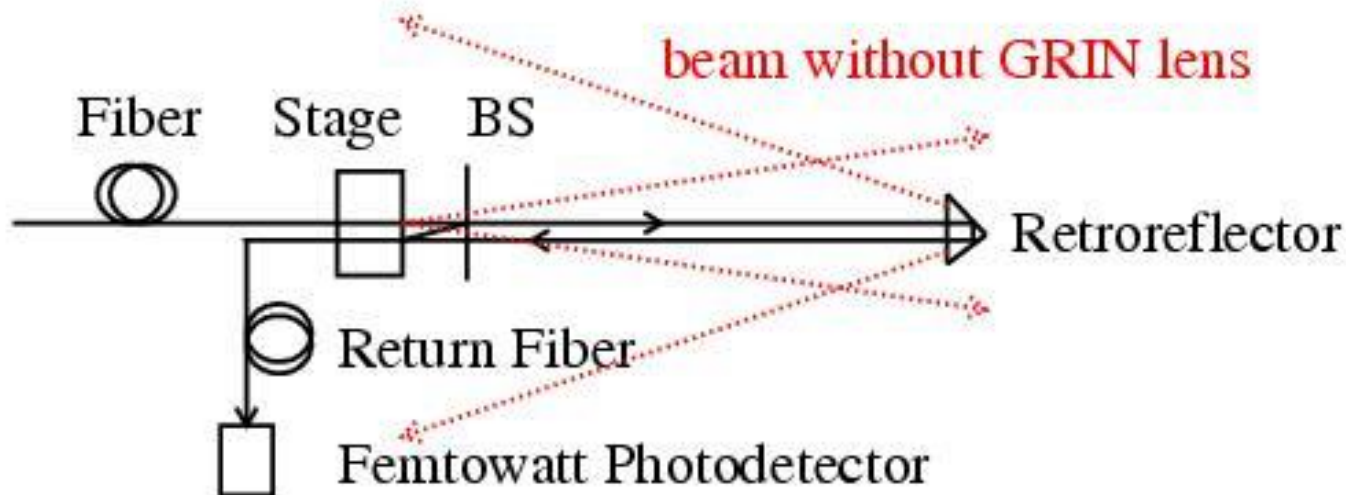
Inside of Box

- ◆ A key issue for the optical fiber FSI is that the intensity of the return beams received by the optical fiber is very weak.

*e.g. the core of the single mode optical fiber has diameter of  $\sim 5 \mu\text{m}$ .*

*Geometrical Efficiency:  $\sim 6.25 \times 10^{-10}$  for a distance of 0.5 m*

- ➔ A novelty in our design is the use of a gradient index lens (GRIN lens – 0.25 pitch lens with  $D=1\text{mm}$ ,  $L=2.58\text{mm}$ ) to collimate the output beam from the optical fiber.
- The density of the outgoing beam is increased by a factor of  $\sim 1000$  by using the GRIN lens. This makes it possible to split the laser beam into many beams to serve a set of interferometers simultaneously.



- If drift error( $\varepsilon$ ) occurs during the laser scanning, it will be magnified by a factor of  $\Omega$  ( $\Omega \equiv v/\Delta v \sim 67$  for full scan of our tunable laser),

$$\text{OPD}^{\text{measured}} = \text{OPD}^{\text{true}} + \Omega\varepsilon$$

➔ *Plastic box and PVC pipes are constructed to reduce thermal drift.*

- Assuming a vibration with one frequency:

$$x_{\text{vib}}(t) = a_{\text{vib}} \times \cos(2\pi f_{\text{vib}}t + \phi_{\text{vib}})$$

- Fringe phase at time t:

$$\Phi(t) = 2\pi \times [\text{OPD}^{\text{true}} + 2x_{\text{vib}}(t)]/\lambda(t)$$

$$\Delta N = [\Phi(t) - \Phi(t_0)]/2\pi = \text{OPD}^{\text{true}} \times \Delta v/c + [2x_{\text{vib}}(t)/\lambda(t) - 2x_{\text{vib}}(t_0)/\lambda(t_0)]$$

- If we assume  $\lambda(t) \sim \lambda(t_0) = \lambda$ , measured OPD can be written as,

$$\text{OPD}^{\text{meas}} = \text{OPD}^{\text{true}} + \Omega \times [2x_{\text{vib}}(t) - 2x_{\text{vib}}(t_0)] \quad (1)$$

$$\text{OPD}^{\text{meas}} = \text{OPD}^{\text{true}} - \Omega \times 4a_{\text{vib}} \sin[\pi f_{\text{vib}}(t-t_0)] \times \sin[\pi f_{\text{vib}}(t+t_0) + \phi_{\text{vib}}] \quad (2)$$

- ➔ Two new multiple-distance measurement techniques are presented to extract vibration and to improve the distance measurement precision based on Eq.1 and Eq.2, respectively.



# Dispersion Effect

- Dispersive elements, beamsplitter, corner cube prism etc. can create significant offset in measured distance for FSI system since the small OPD change caused by dispersion is magnified by a factor of  $\Omega$ .

- Sellmeier formula for dispersion in crown glass (BK7)

$$n^2(\lambda^2) = 1 + B1 * \lambda^2 / (\lambda^2 - C1) + B2 * \lambda^2 / (\lambda^2 - C2) + B3 * \lambda^2 / (\lambda^2 - C3)$$

$$B1 = 1.03961212, B2 = 0.231792344, B3 = 1.01046945$$

$$C1 = 0.00600069867, C2 = 0.0200179144, C3 = 103.560653$$

- Numerical simulation results (**thickness of the corner cube prism = 1.86 cm**)

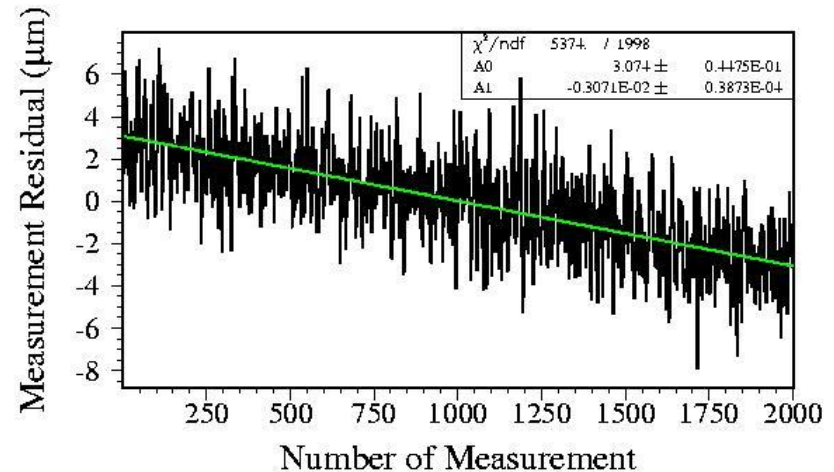
$$R_1 - R_{\text{true}} = 373.876 \text{ um}, R_{2000} - R_{\text{true}} = 367.707 \text{ um}$$

$$R_1 - R_{2000} = 6.2 \text{ +/- } 0.2 \text{ um}$$

- Real data - fitted result

$$R_1 - R_{2000} = 6.14 \text{ +/- } 0.1 \text{ um}$$

- ➔ Dispersion effects can be avoided by using hollow retroreflector and put the beamsplitter's anti-reflecting surface facing the optical fiber.





# Error Estimations

- Error from uncertainties of fringe and frequency determination,  $dR/R \sim 1.9$  ppm; if  $N_{\text{meas}} = 1200$ ,  $dR/R \sim 77$  ppb
- Error from vibration.  $dR/R \sim 0.4$  ppm; if  $N_{\text{meas}} = 1200$ ,  $dR/R \sim 10$  ppb
- Error from thermal drift. Temperature fluctuations are well controlled down to 0.5 mK(RMS) in Lab by plastic box on optical table and PVC pipes shielding the volume of air near the laser beam. An air temperature change of 1 °C will result in a 0.9 ppm change of refractive index at room temperature. The drift will be magnified during scanning. if  $N_{\text{meas}} = 1200$ ,  $dR/R \sim 0.9$  ppm/K  $\times$  0.5mK  $\times$   $\Omega(94) \sim 42$  ppb.
- Error from air humidity and pressure,  $dR/R \sim 10$  ppb.

**The total error from the above sources is  $\sim 89$  ppb which agrees well with the measured residual spread of  $\sim 90$  ppb over different days and times of measurement.**

Measured Distances: 10 cm – 60 cm

Controlled  
Conditions

Distance Precision:

~ 50 nm by using multiple-distance measurement technique under well controlled laboratory conditions.

Vibration Measurement:

0.1-100 Hz, amplitude as low as few nanometers, can be extracted precisely using new vibration extraction technique.

Publication:

*“High-precision absolute distance and vibration measurement with frequency scanned interferometry”*, [Physics/0409110]

H.J. Yang, J. Deibel, S. Nyberg, K. Riles, *Applied Optics*, 44, 3937-44, (2005)

- ➔ Used a Micrometer to change the position of retroreflector by large amount (127+/- 3 microns), and check FSI performance.  
The measurement precision is ~ 0.5 microns with unstable temperature.
  
- ➔ Used a Piezoelectric transducer (PZT, 20% tolerance) to change the position of the retroreflector by 2.0 +/- 0.4 microns.  
The measurement precision is ~ 0.1 microns with stable temperature.
  
- ➔ To verify correct tracking of large thermal drifts, we placed a heating pad on a 1' x 2' x 0.5'' Al breadboard to increase temperature by 4 ~ 7 °C.  
The measured thermal expansions agree well with expectations, the measurement precision is ~ 0.2 microns.

→ Used a Micrometer to change the position of retroreflector by large amount (127+/- 3 microns), and check FSI performance. Laser #1, 5 full scan data for each independent test.

$$dR1 = 128.68 \pm 0.46 \text{ microns}$$

$$dR2 = 129.55 \pm 0.63 \text{ microns}$$

$$dR3 = 127.44 \pm 0.63 \text{ microns}$$

$$dR4 = 124.90 \pm 0.48 \text{ microns}$$

Single-laser scans –  
unstable temps

→ Used a Piezoelectric transducer (PZT, 20% tolerance) to change the position of the retroreflector by 2.0 +/- 0.4 microns. Laser #1, 5 full scans for each test.

$$dR5 = 2.33 \pm 0.12 \text{ microns}$$

$$dR6 = 2.23 \pm 0.07 \text{ microns}$$

Single-laser scans –  
stable temps

- To verify correct tracking of large thermal drifts, we placed a heating pad on a 1' X 2' X 0.5'' Aluminum breadboard
  - ➔ Test 1: increased temperature by 6.7 +/- 0.1 °C
    - dR\_expected = 62.0 +/- 0.9 microns
    - dR\_measured = 61.72 +/- 0.18 microns
  - ➔ Test 2: increased temperature by 6.9 +/- 0.1 °C
    - dR\_expected = 64.4 +/- 0.9 microns
    - dR\_measured = 64.01 +/- 0.23 microns
  - ➔ Test 3: increased temperature by 4.3 +/- 0.1 °C
    - dR\_expected = 39.7 +/- 0.9 microns
    - dR\_measured = 39.78 +/- 0.22 microns
  - ➔ Test 4: increased temperature by 4.4 +/- 0.1 °C
    - dR\_expected = 40.5 +/- 0.9 microns
    - dR\_measured = 41.02 +/- 0.21 microns

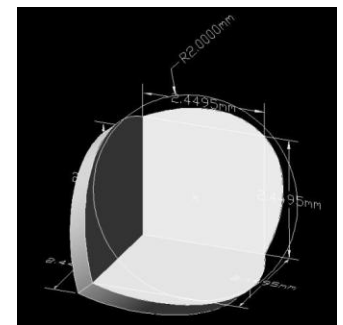
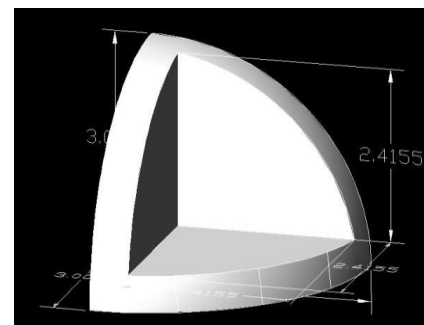
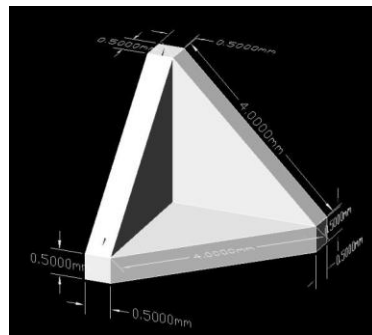
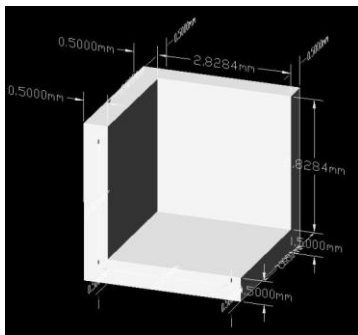
Dual-laser scans  
– closed box

Previously used large commercial optics:

- Retroreflector (Diameter ~ 1'')
- Beam splitter (Diameter ~ 1'')

Need miniaturized, low- $X_0$  components for actual tracker

Obtained customized fabrication quotes for retroreflectors (3~4 mm) from rapid prototyping companies.





→ Cheap prototype alternatives: a bicycle reflector:  
(all but one pixel masked off)



Measurement precision for a distance of 18 cm:  $\sim 0.4 \mu\text{m}$

Promising indication, given simple design of the reflector pixels  
( solid plastic corner cubes with no coating,  
but low reflective efficiency )

# Miniaturization



- Now using Edmund corner cube array, 9 X 9 hexagon corner cubes in 35 mm X 35 mm. Center-to-center spacing of two adjacent corner cubes is ~ 4 mm.
- The reflective efficiency of single corner cube is comparable to large commercial corner cube and hollow retroreflector ( D = 1 inch ).
- High reflective efficiency is vital to make qualified fringes and to make more channels.
- Under controlled conditions  
 $L = 417198.37 \pm 0.07$  microns
- The corner cube array has high reflective efficiency and qualified fringes. It's very promising.



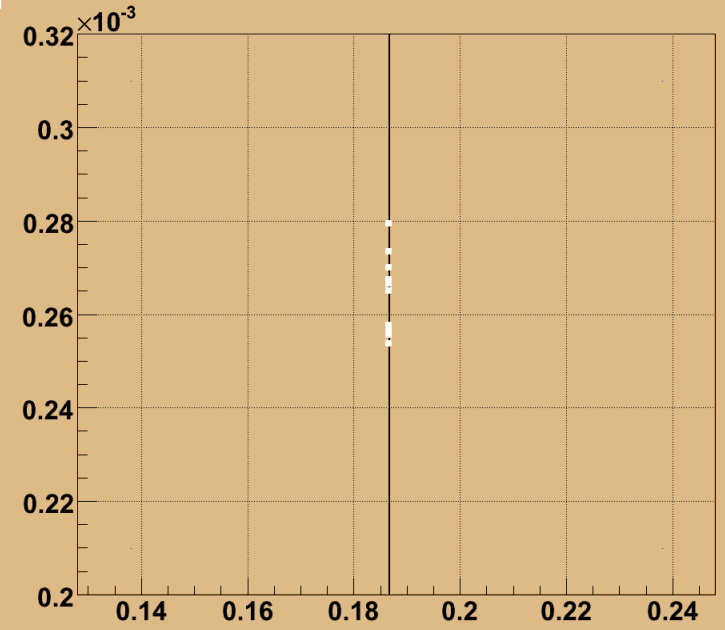
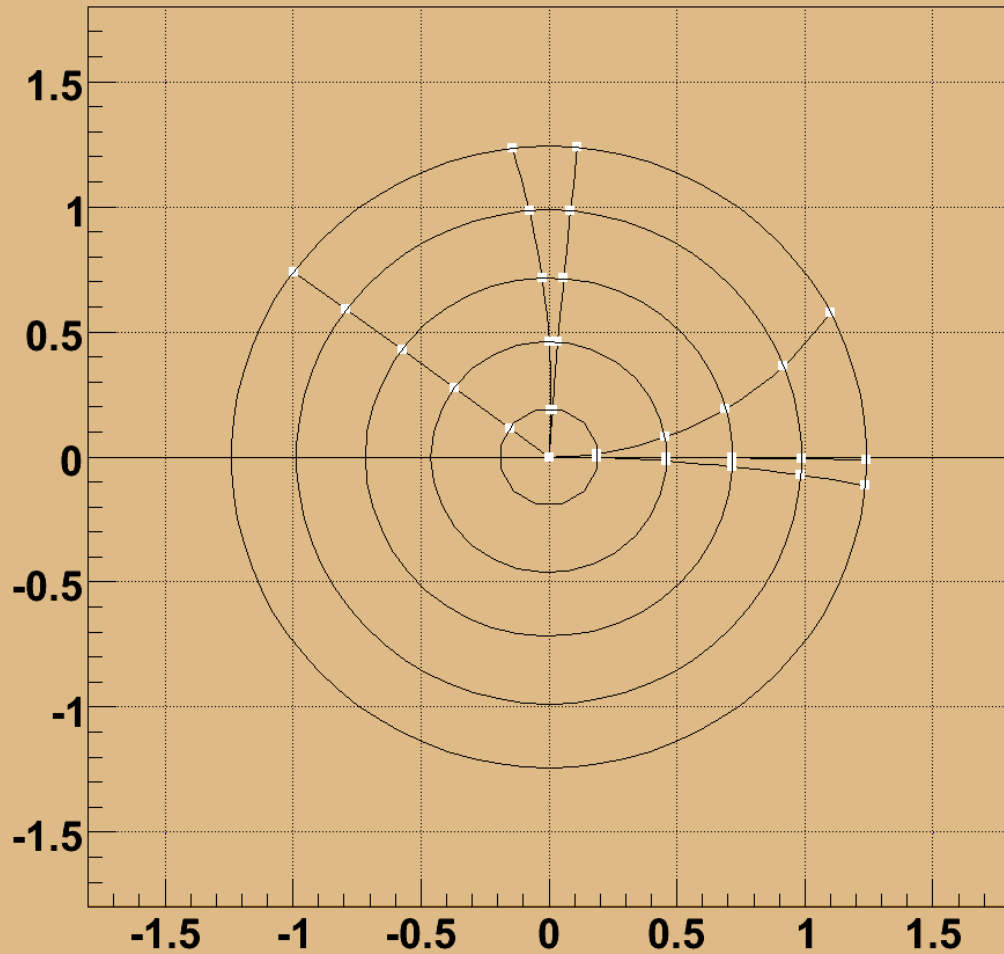
## Dual-Laser FSI Data Samples – Under Realistic Conditions

- \* with box open(20 scans), with fan on (10 scans), with vibration(8 scans).
- \* Scanning rates for Laser #1 and #2 are -0.4 and 0.4 nm/s, respectively.
- \* Scanning time is 25 seconds, sampling rate is 100 KS/s.
- \* Two lasers are operated simultaneously, 2-blade chopper frequency is 20 Hz.

Data	Scans	Conditions	Distance(cm) from dual-laser	Precision( $\mu\text{m}$ ) for multi-dist.-meas./scan					
				2000	1500	1000	500	100	1
L1	10	open box	–	5.70	5.73	6.16	6.46	5.35	6.64
L2	10	open box	–	5.73	5.81	6.29	6.61	5.66	6.92
L1+L2	10	open box	41.13835	0.20	0.19	0.18	0.21	0.39	1.61
L1	10	open box+fan on	–	5.70	4.91	3.94	3.49	3.29	3.04
L2	10	open box+fan on	–	5.70	5.19	4.23	3.78	3.21	6.07
L1+L2	10	open box+fan on	41.13841	0.19	0.17	0.20	0.22	0.31	3.18
L1	10	open box	–	6.42	5.53	4.51	3.96	4.41	3.36
L2	10	open box	–	6.81	5.93	4.86	4.22	4.63	5.76
L1+L2	10	open box	41.13842	0.20	0.20	0.26	0.19	0.27	2.02
L1	8	open box+vibration	–	4.73	4.82	3.60	3.42	4.62	8.30
L2	8	open box+vibration	–	4.72	4.66	3.66	3.65	4.63	5.56
L1+L2	8	open box+vibration	41.09524	0.17	0.21	0.17	0.15	0.39	1.75

- To evaluate the impact of distortion of silicon ladder on charged track momentum reconstruction/measurement.
- Integrated track generation, reconstruction and FSI fitting
- Inputs: charged track with given momentum, 5 silicon layers based on nominal SiD design, magnetic field  $B = 5$  Tesla.
  - Assume spatial resolution is 7 microns for hits.
  - Distortions: rotations, translations, thermal expansion or contractions of silicon ladders.
  - Applying FSI line-of-sight grid constraint  
(code not fully debugged – premature to show results,  
but consistent with earlier simulations.)
- Outputs: reconstructed momentum of charged track,  
event displays for SiD Tracker

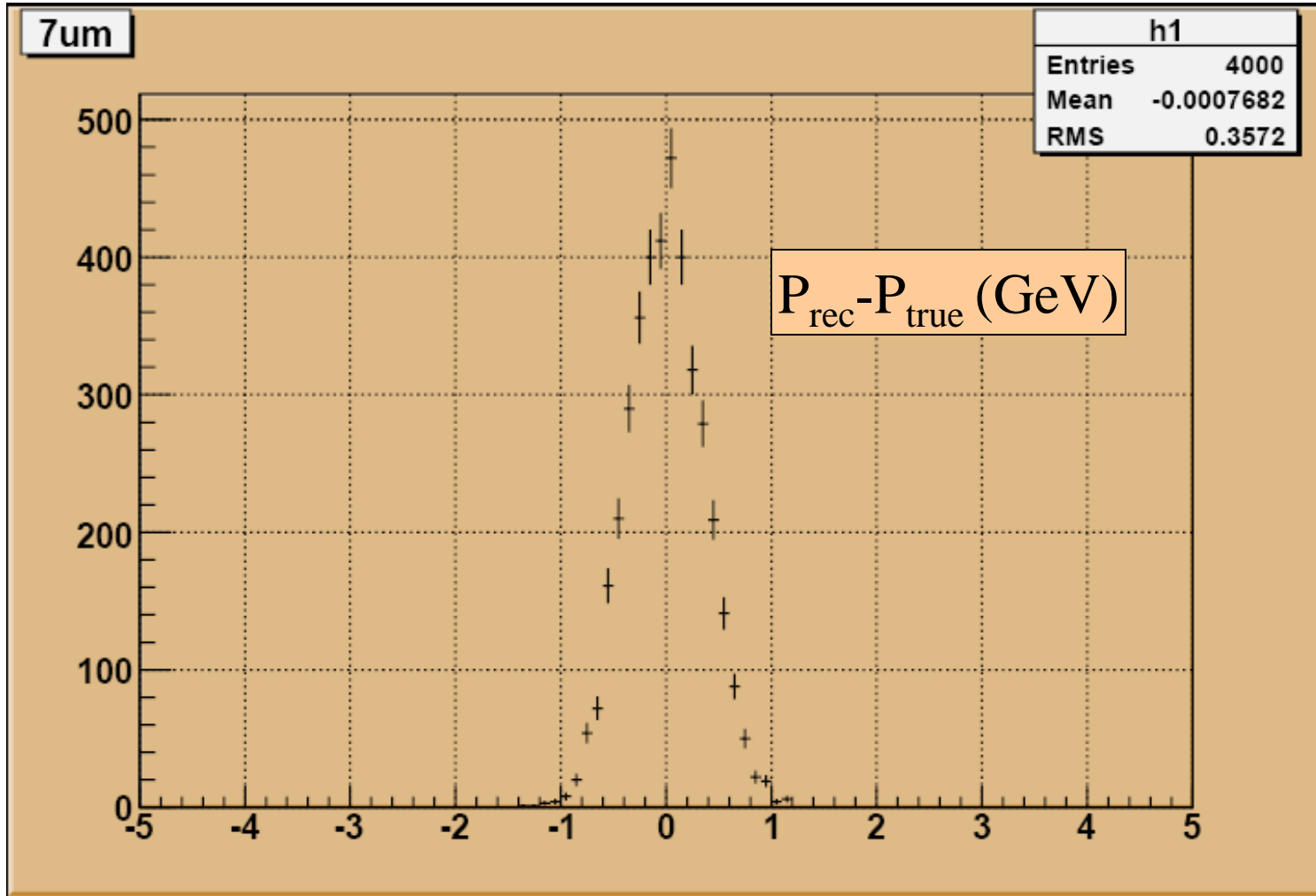
# Example Tracks (side view)



Can zoom in on specific locations

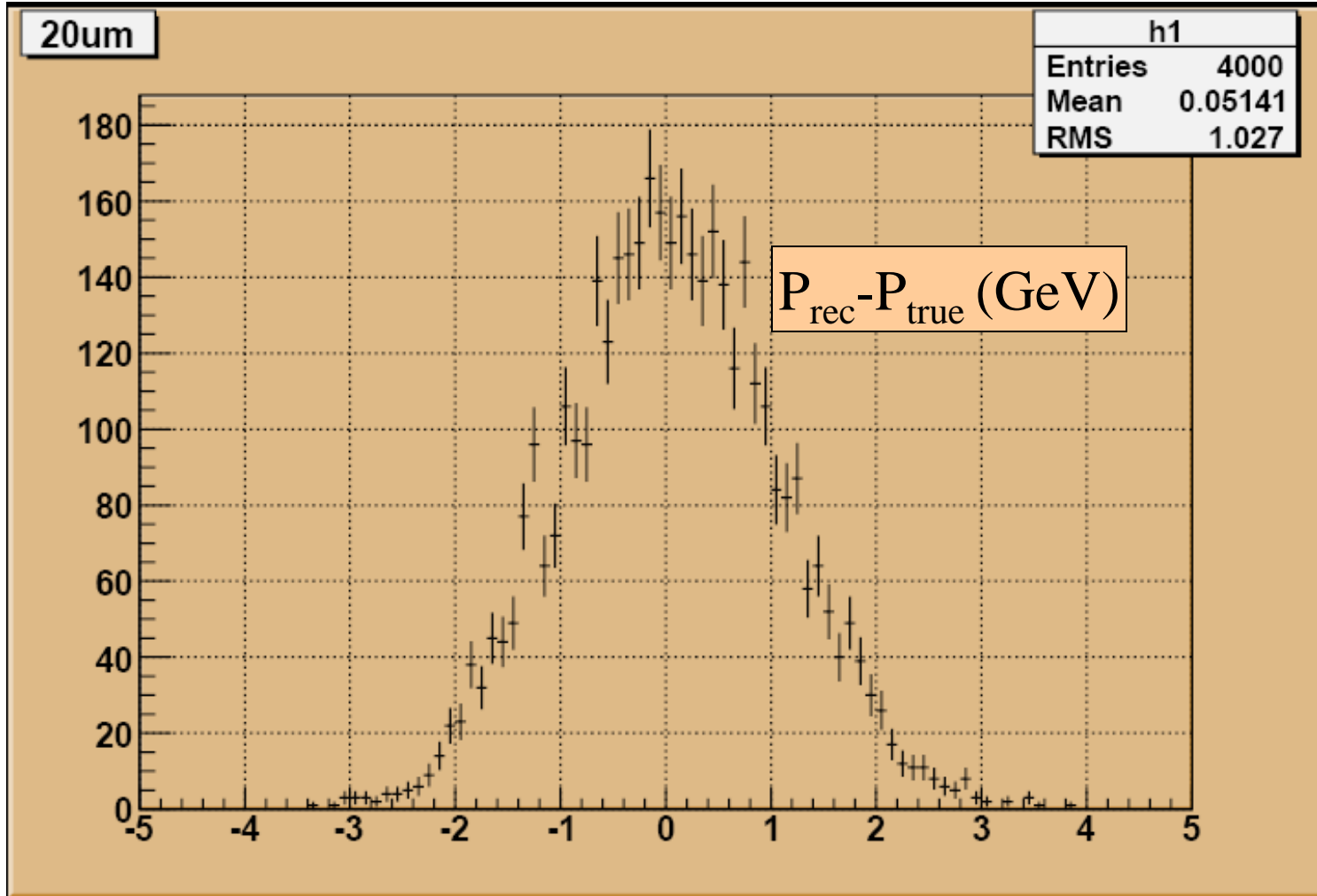


# Normal ( $\sigma = 7$ microns for hits)

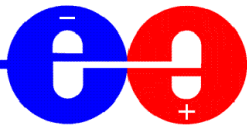


$P_{\text{true}} = 100$  GeV, hit smearing  $\sim 7$  microns

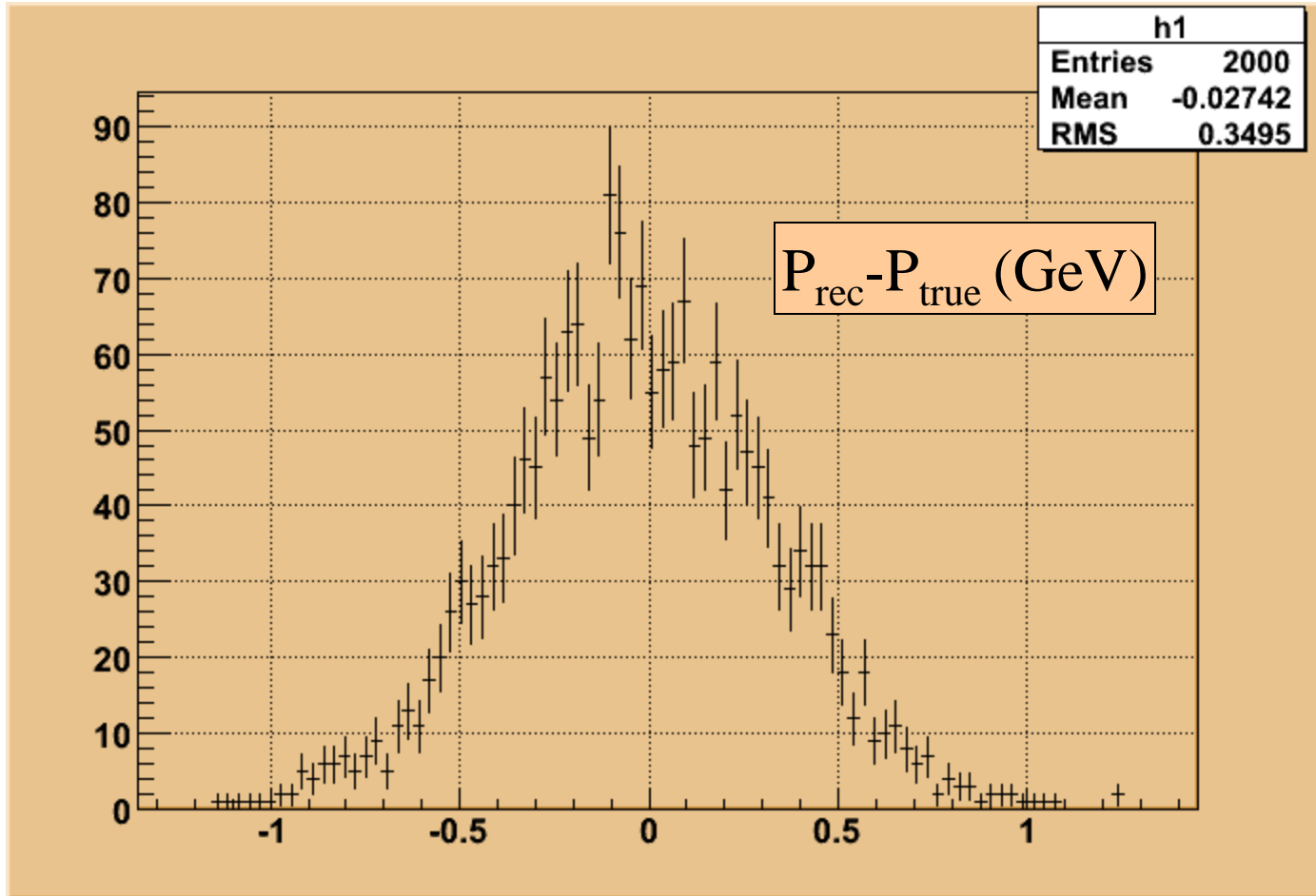
# Normal ( $\sigma = 20$ microns for hits)



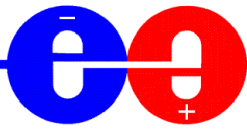
$P_{\text{true}} = 100$  GeV, hit smearing  $\sim 20$  microns



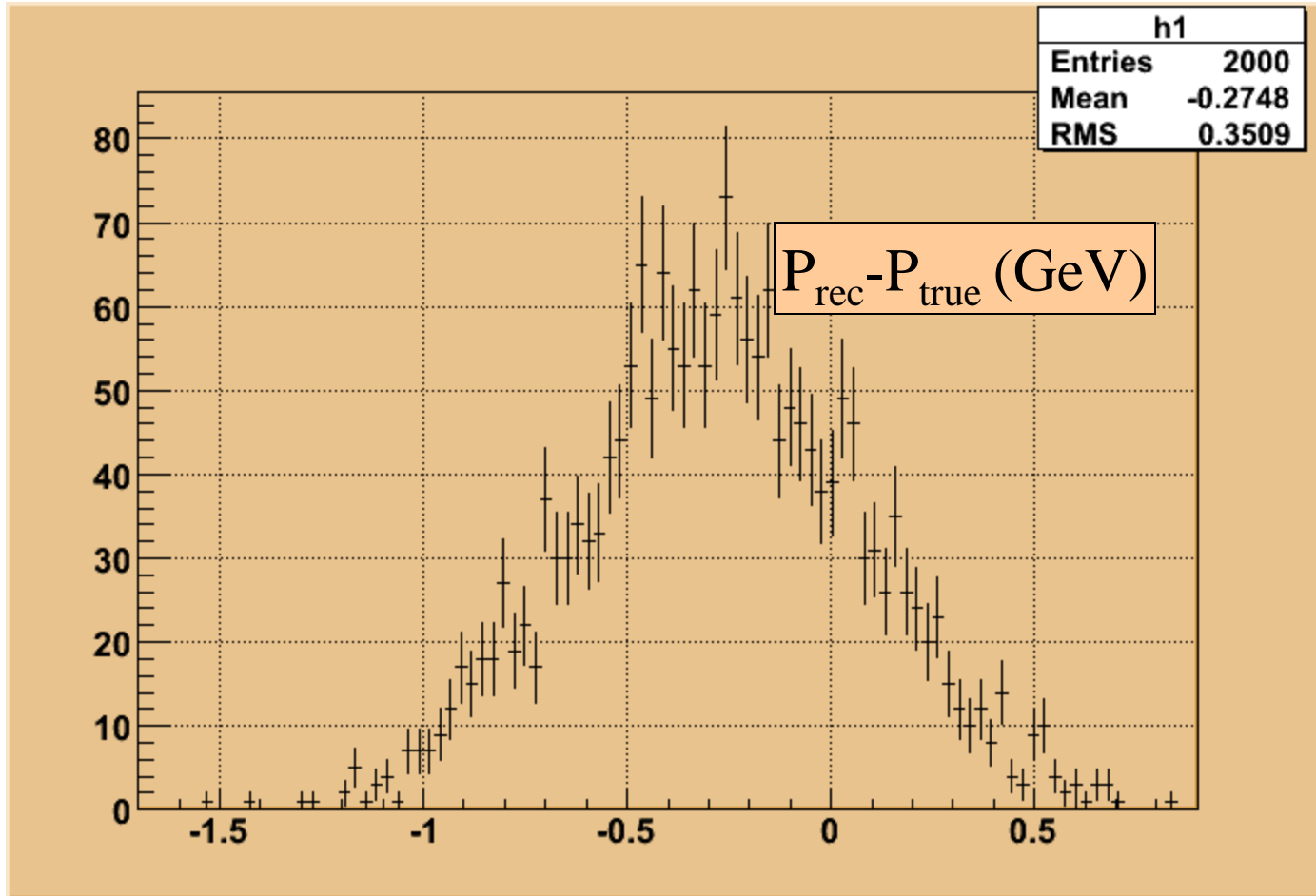
# Translation of Silicon Ladder (Middle)



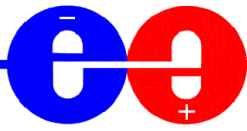
$P_{\text{true}} = 100 \text{ GeV}$ , shift  $\sim 1 \text{ micron}$



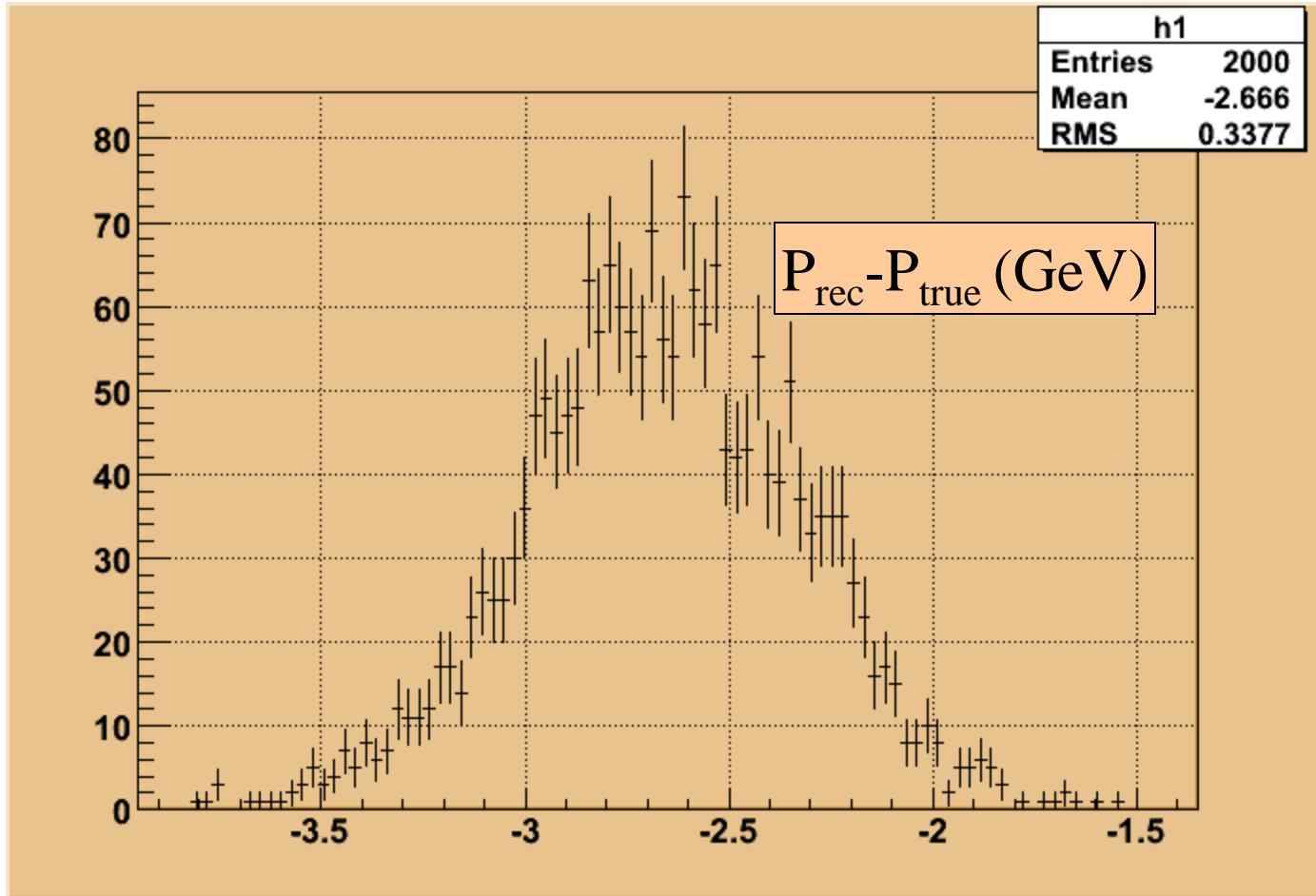
# Translation of Silicon Ladder (Middle)



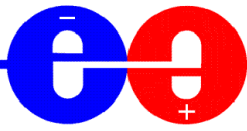
$P_{\text{true}} = 100$  GeV, shift  $\sim 10$  microns



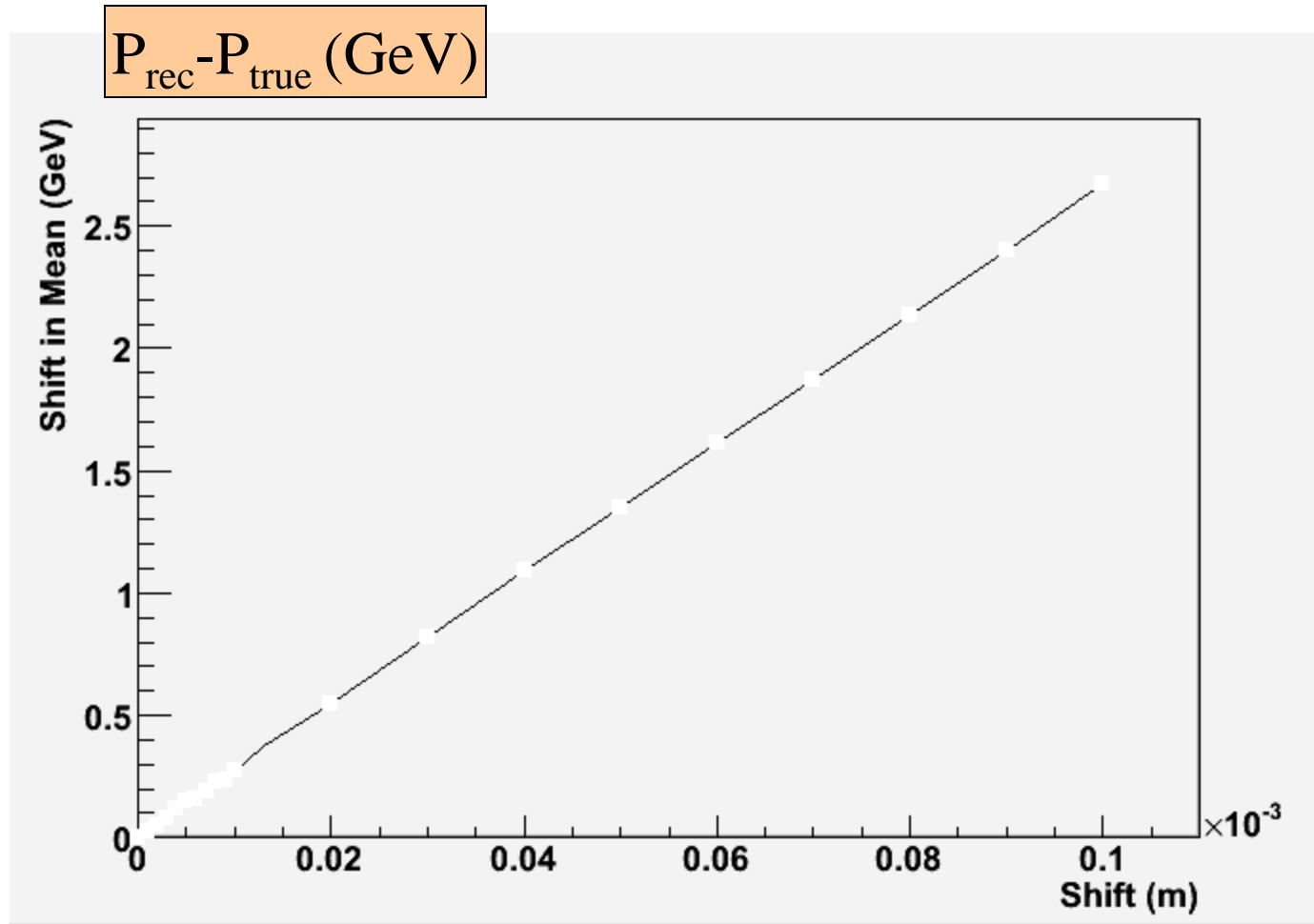
# Translation of Silicon Ladder (Middle)



$P_{\text{true}} = 100 \text{ GeV}$ , shift  $\sim 100 \text{ microns}$



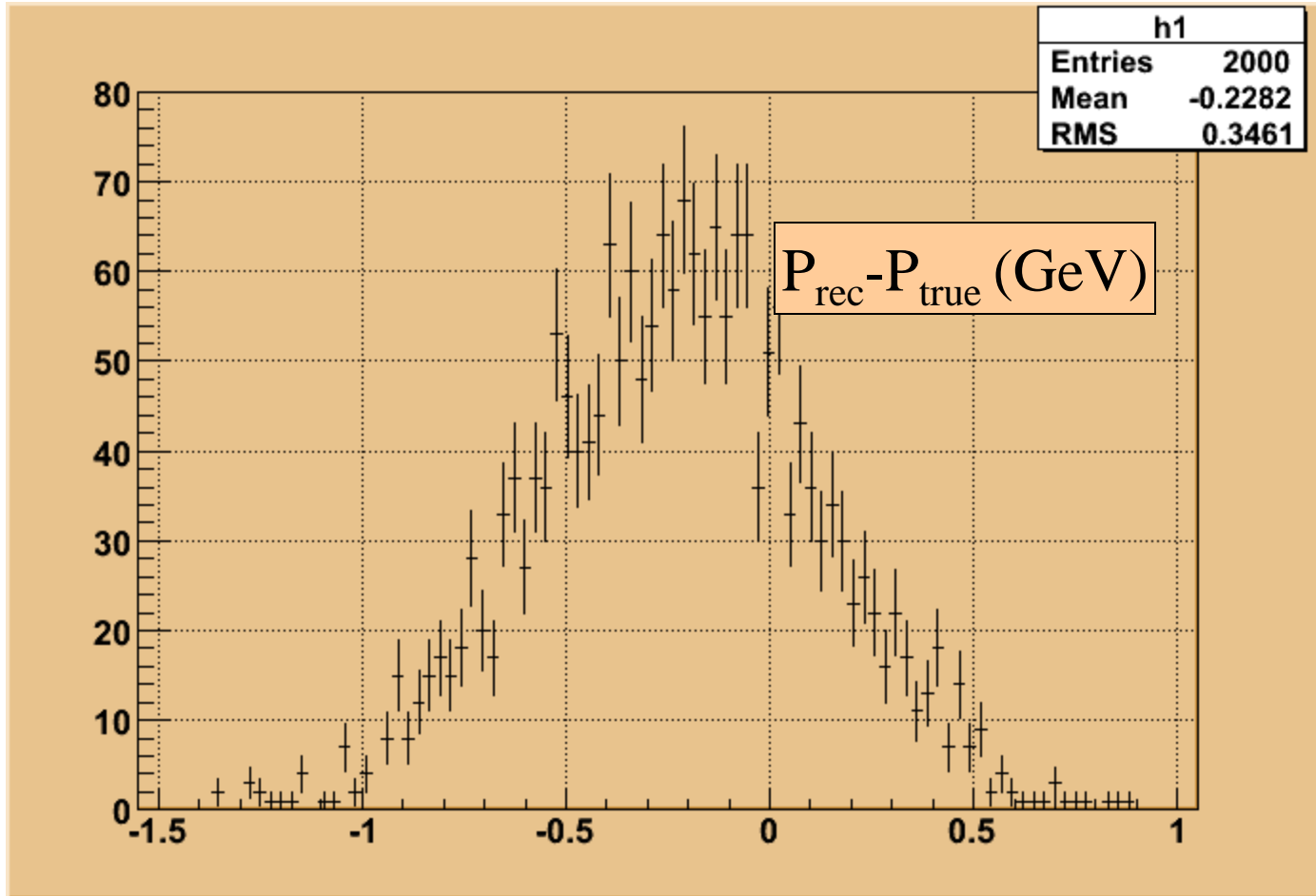
# Translation of Silicon Ladder (Middle)



$P_{\text{true}} = 100 \text{ GeV}$ , shift  $\sim 10 - 100 \text{ microns}$



# Rotation of Silicon Ladder (Middle)



$P_{\text{true}} = 100 \text{ GeV, Rotate } \sim 1 * 10^{-5} \text{ rad}$

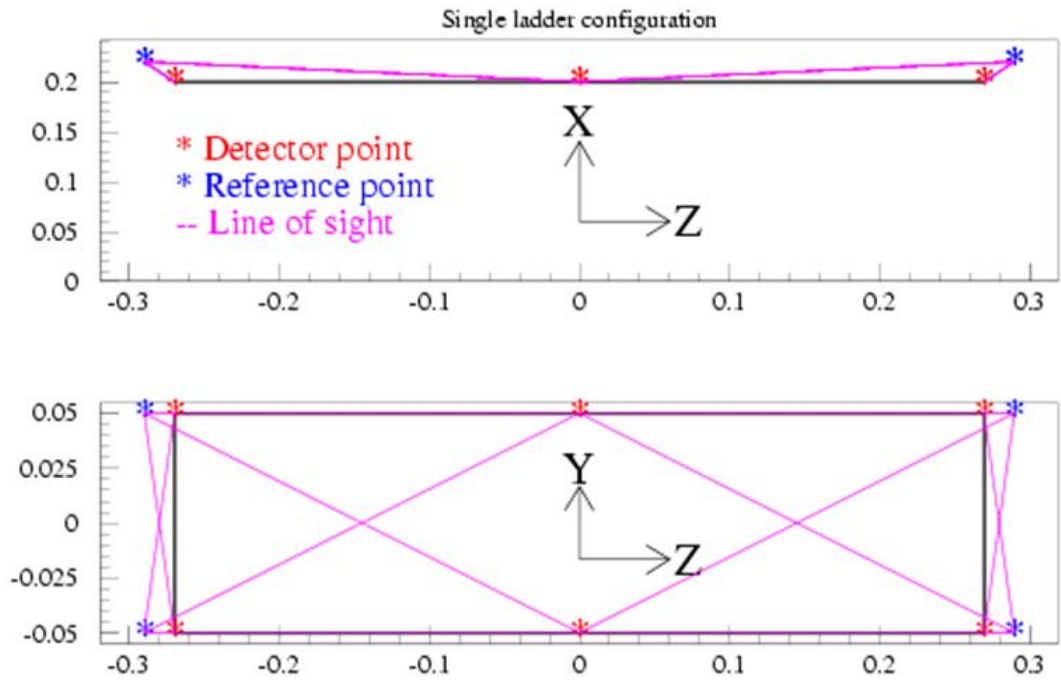
# Systematic Error Estimations

- \* The major systematic bias comes from uncertainty of the Free Spectral Range (FSR) of the Fabry Perot interferometer used to determine scanned frequency range precisely, the relative error would be  $dR/R \sim 50$  ppb if the FSR was calibrated by an wavemeter with a precision of 50 ppb. A wavemeter of this precision was not available for the measurement described here.
- \* The systematic bias from the multiple-distance-measurement technique was also estimated by changing the starting point of the measurement window, the window size and the number of measurements, the uncertainties typically range from 10-30 nanometers ( $< 50$  ppb).
- \* The systematic bias from uncertainties of temperature, air humidity and barometric pressure scales should have negligible effect.

**The total systematic error is  $\sim 70$  ppb.**

- Will eventually use hundreds of distance measurements along lines of sight to determine tracking component positions, rotations (**pitch/roll/yaw**), and internal distortions.
- System simulations starting – first steps with **rigid bodies**:
  - **Align single silicon ladder**
  - **Align single cylinder (e.g., Si disk, TPC, or CCD cryostat)**
- Assumes (for now) distance resolution of 0.5 microns for all lines of sight [**optimistic for  $d > 1$  meter, conservative otherwise**]
- Assumes rigid supports for off-tracker reference points and known positions of reference points [**from combination of surveying and triangulation between reference points**]

# Alignment of Single Silicon Ladder



Ladder dimensions

Radius = 20.0 cm

Half-length = 27.0 cm

Width = 10.0 cm

Refer. offsets from ladder ends

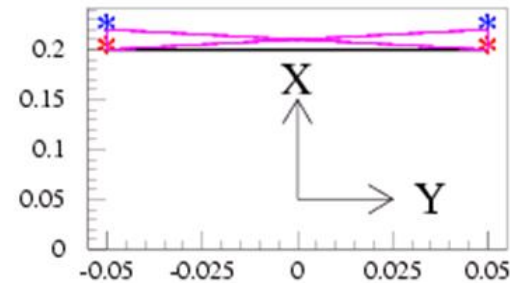
$r = 2.0$  cm  $z = 2.0$  cm

CM position precisions ( $\mu\text{m}$ )

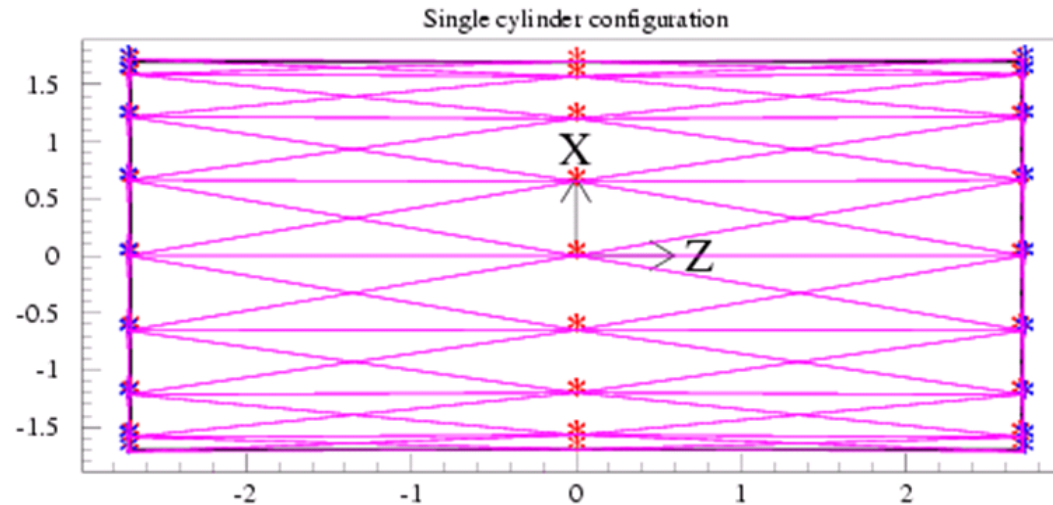
$x = 0.3$   $y = 0.3$   $z = 0.2$

Axis rotation precisions ( $\mu\text{rad}$ )

$\psi = 0.9$   $\theta = 1.4$   $\phi = 7.0$



# Alignment of Single TPC Cylinder



\* Detector point  
\* Reference point  
-- Line of sight

Cylinder dimensions

Radius = 1.70 m

Half-length = 2.70 m

Refer. offsets from cylinder ends

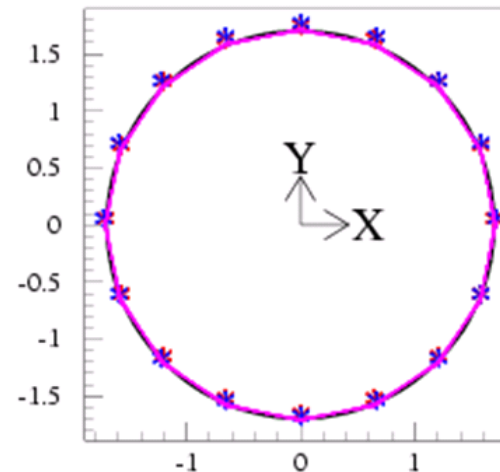
$r = 2.0$  cm  $z = 2.0$  cm

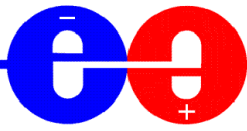
CM position precisions ( $\mu\text{m}$ )

$x = 0.08$   $y = 0.06$   $z = 0.05$

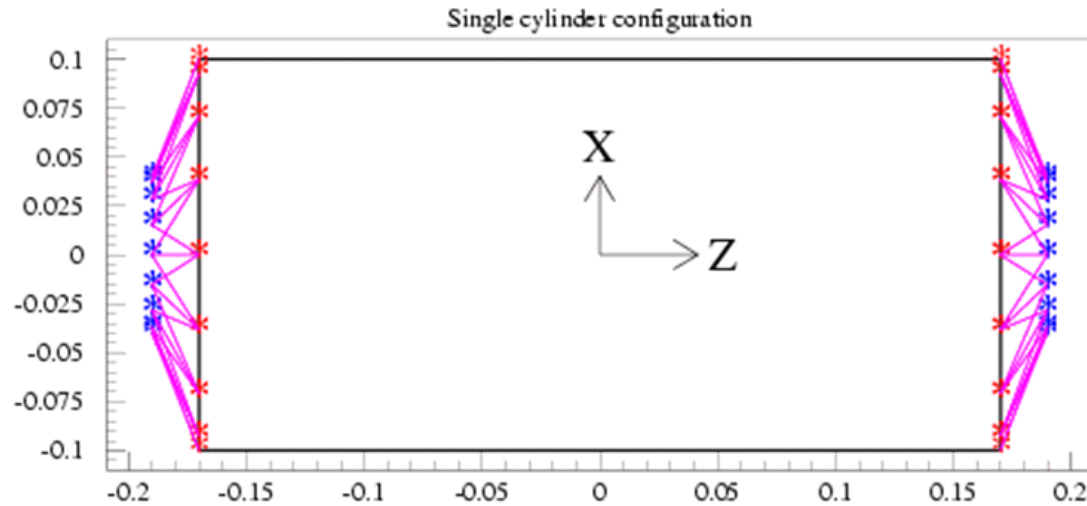
Axis rotation precisions ( $\mu\text{rad}$ )

$\psi = 0.02$   $\theta = 0.02$   $\phi = 0.03$





# Alignment of Single CCD Cylinder



- \* Detector point
- \* Reference point
- Line of sight

Cylinder dimensions

Radius = 0.10 m

Half-length = 0.17 m

Refer. offsets from cylinder ends

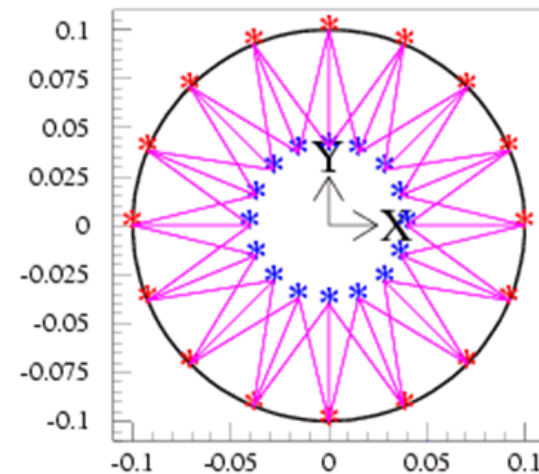
$r = -6.0$  cm  $z = 2.0$  cm

CM position precisions ( $\mu$ m)

$x = 0.08$   $y = 0.08$   $z = 0.17$

Axis rotation precisions ( $\mu$ rad)

$\psi = 0.38$   $\theta = 0.38$   $\phi = 2.77$





- ➔ Simulate internal distortions:
  - Thermal expansion
  - Mechanical deformations (e.g., twist, sag)
- ➔ Simultaneous fit to multiple tracker components
- ➔ Address systematic errors from reference point uncertainties (and possible drifts)
- ➔ Propagate uncertainties from ladder/cylinder position, orientation, distortion to errors on track hits and evaluate gain in momentum / impact parameter resolution from alignment corrections